AGU PUBLICATIONS

JGR

Journal of Geophysical Research: Atmospheres

RESEARCH ARTICLE
10.1002/2015JD023638

Key Points:
- The 2014–2015 Icelandic fissure eruption at Bárðarbunga affected air quality in far field
- Satellite-derived average daily SO_2 burden of 99 ± 49 kt (OMI) and 61 ± 18 kt (IASI) in September 2014
- We calculate a total release of 2.0 ± 0.6 Tg of SO_2 for September 2014 and fluxes up to 120 kt/d

Supporting Information:
- Figures S1–S4 and Tables S1–S4 captions
- Figure S1
- Figure S2
- Figure S3
- Figure S4
- Table S1
- Table S2
- Table S3
- Table S4

Correspondence to:
A. Schmidt,
a.schmidt@leeds.ac.uk

Citation:
Schmidt, A., et al. (2015), Satellite detection, long-range transport, and air quality impacts of volcanic sulfur dioxide from the 2014–2015 flood lava eruption at Bárðarbunga (Iceland), *J. Geophys. Res. Atmos.*, *120*, doi:10.1002/2015JD023638.

Received 5 MAY 2015
Accepted 18 AUG 2015
Accepted article online 21 AUG 2015

Satellite detection, long-range transport, and air quality impacts of volcanic sulfur dioxide from the 2014–2015 flood lava eruption at Bárðarbunga (Iceland)

Anja Schmidt[1], Susan Leadbetter[2], Nicolas Theys[3], Elisa Carboni[4], Claire S. Witham[2], John A. Stevenson[5], Cathryn E. Birch[2], Thorvaldur Thordarson[6], Steven Turnock[1], Sara Barsotti[7], Lin Delaney[8], Wuhu Feng[9], Roy G. Grainger[4], Matthew C. Hort[2], Ármann Höskuldsson[6], Iolanda Ialongo[10], Evgenia Ilyinskaya[11], Thorsteinn Jóhannsson[12], Patrick Kenny[8], Tamsin A. Mather[13], Nigel A. D. Richards[1], and Janet Shepherd[14]

[1]School of Earth and Environment, University of Leeds, Leeds, UK, [2]Met Office, Exeter, UK, [3]Belgian Institute for Space Aeronomy, Brussels, Belgium, [4]COMET, Atmospheric, Oceanic and Planetary Physics, University of Oxford, Oxford, UK, [5]School of GeoSciences, Grant Institute, University of Edinburgh, Edinburgh, UK, [6]Faculty of Earth Sciences, Institute of Earth Sciences and Nordvulk, University of Iceland, Reykjavik, Iceland, [7]Icelandic Met Office, Reykjavik, Iceland, [8]Environmental Protection Agency, Dublin, Ireland, [9]National Centre for Atmospheric Science, University of Leeds, Leeds, UK, [10]Earth Observation Unit, Finnish Meteorological Institute, Helsinki, Finland, [11]British Geological Survey, Edinburgh, UK, [12]Environment Agency of Iceland, Reykjavík, Iceland, [13]COMET, Department of Earth Sciences, University of Oxford, Oxford, UK, [14]Scottish Environment Protection Agency, Holytown, UK

Abstract The 2014–2015 Bárðarbunga-Veiðivötn fissure eruption at Holuhraun produced about 1.5 km^3 of lava, making it the largest eruption in Iceland in more than 200 years. Over the course of the eruption, daily volcanic sulfur dioxide (SO_2) emissions exceeded daily SO_2 emissions from all anthropogenic sources in Europe in 2010 by at least a factor of 3. We present surface air quality observations from across Northern Europe together with satellite remote sensing data and model simulations of volcanic SO_2 for September 2014. We show that volcanic SO_2 was transported in the lowermost troposphere over long distances and detected by air quality monitoring stations up to 2750 km away from the source. Using retrievals from the Ozone Monitoring Instrument (OMI) and the Infrared Atmospheric Sounding Interferometer (IASI), we calculate an average daily SO_2 mass burden of 99 ± 49 kilotons (kt) of SO_2 from OMI and 61 ± 18 kt of SO_2 from IASI for September 2014. This volcanic burden is at least a factor of 2 greater than the average SO_2 mass burden between 2007 and 2009 due to anthropogenic emissions from the whole of Europe. Combining the observational data with model simulations using the United Kingdom Met Office's Numerical Atmospheric-dispersion Modelling Environment model, we are able to constrain SO_2 emission rates to up to 120 kilotons per day (kt/d) during early September 2014, followed by a decrease to 20–60 kt/d between 6 and 22 September 2014, followed by a renewed increase to 60–120 kt/d until the end of September 2014. Based on these fluxes, we estimate that the eruption emitted a total of 2.0 ± 0.6 Tg of SO_2 during September 2014, in good agreement with ground-based remote sensing and petrological estimates. Although satellite-derived and model-simulated vertical column densities of SO_2 agree well, the model simulations are biased low by up to a factor of 8 when compared to surface observations of volcanic SO_2 on 6–7 September 2014 in Ireland. These biases are mainly due to relatively small horizontal and vertical positional errors in the simulations of the volcanic plume occurring over transport distances of thousands of kilometers. Although the volcanic air pollution episodes were transient and lava-dominated volcanic eruptions are sporadic events, the observations suggest that (i) during an eruption, volcanic SO_2 measurements should be assimilated for near real-time air quality forecasting and (ii) existing air quality monitoring networks should be retained or extended to monitor SO_2 and other volcanic pollutants.

1. Introduction

Between 31 August 2014 and 28 February 2015, a spectacular fissure eruption of the Bárðarbunga-Veiðivötn volcanic system took place at the Holuhraun lava field in Iceland. The eruption was preceded by 2 weeks of intense seismic activity located at the caldera of Bárðarbunga central volcano [*Gudmundsson et al.*, 2014; *Sigmundsson et al.*, 2015]. The vents of the 2014–2015 eruption (Figure 1) are located on the outwash plains of the Dyngjujökull glacier (at the northern edge of Vatnajökull glacier) and reoccupied the vents of the

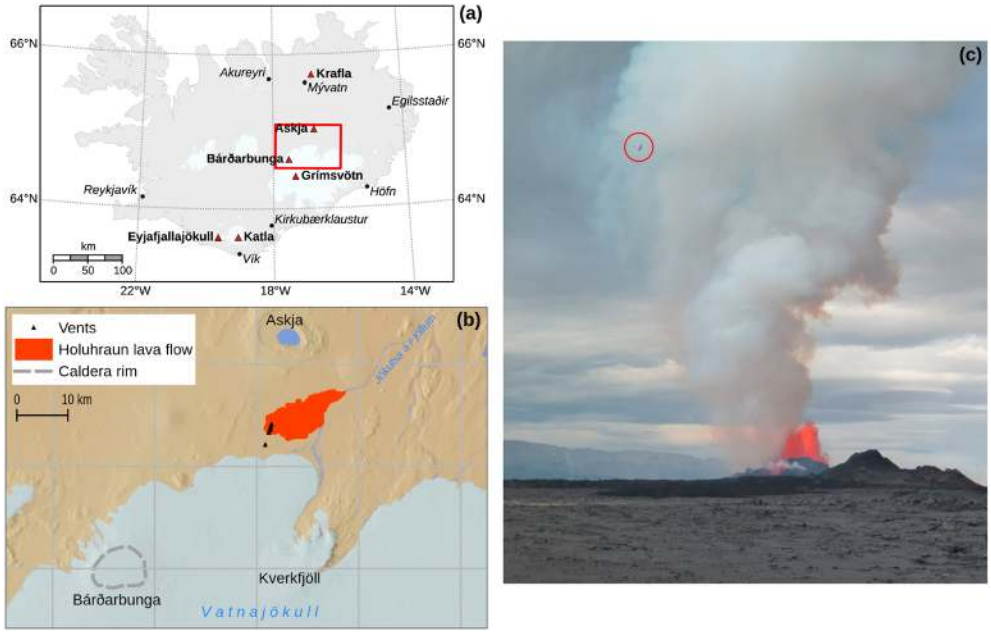

Figure 1. Overview of the 2014–2015 eruption at Holuhraun showing (a) the locations of the Icelandic towns and volcanoes, including the Bárðarbunga-Veiðivötn volcanic system. The red rectangle outlines the region shown in Figure 1b. (b) Map showing the Bárðarbunga caldera (dashed gray line) and the lava flow field and vents of the 2014–2015 eruption. The extent of the lava flow was digitized from a SENTINEL radar image produced by the University of Iceland. Vent locations have been drawn from Operational Land Imager (on Landsat 8) acquired on 6 September 2014. (c) Looking north at the 2014–2015 vents on 13 September 2014. The craters are around 50 m high; fire fountains reach heights of 100 m. The plume rising from the vent is rich in water vapor, sulfur dioxide, and other gases but contains very little volcanic ash. Light aircraft (circled) for scale.

Holuhraun lava erupted in 1797 and 1862–1864 [*Hartley and Thordarson*, 2013]. During early September 2014, the effusive (i.e., lava-producing) eruption of basalt magma was characterized by 100 m high fire fountains along a 1.5 km long fissure producing very little tephra. By mid-September 2014, the activity gradually became limited to four craters eventually forming a 400 m long lava pond by mid-November 2014.

The 2014–2015 lava flow field covers about 85 km^2 extending northeast from the vent system toward the Jökulsá á Fjöllum River (Figure 1) and is as yet unnamed. For convenience, we refer to the eruption as the 2014–2015 eruption at Holuhraun in this paper. Based on the area and thickness of the lava flow field, a lava discharge rate of 200–280 m^3/s has been estimated for early September 2014 [*Höskuldsson et al.*, 2015]. After 11 September 2014 the discharge declined to 140–250 m^3/s, and by November 2014 it reduced further to 10–100 m^3/s [*Dürig et al.*, 2015; *Höskuldsson et al.*, 2015]. The total volume of lava produced by the 2014–2015 eruption is about 1.5 km^3 [*Icelandic Met Office* (*IMO*), 2015]. According to the definition used in *Thordarson and Larsen* [2007], the 2014–2015 eruption at Holuhraun is therefore the first Icelandic *flood lava eruption* since the 1783–1784 Common Era (C.E.) Laki eruption.

Ground-based and satellite remote sensing showed that the eruption continuously emitted large amounts of sulfur dioxide (SO_2) into the troposphere with plumes reaching heights of 1–3 km on average [*Arason et al.*, 2015]. Ground-based optical remote sensing and lava discharge rates combined with petrological estimates of the gas release suggest average emission rates of 35 kilotons per day (kt/d) over the course of the eruption [*IMO*, 2015] and up to 120 kt/d during September 2014 [*Thordarson and Hartley*, 2015]. Therefore, the 2014–2015 eruption emitted at least 3 times more SO_2 per day than the total of all anthropogenic SO_2 sources (including domestic shipping) in 28 European countries in 2010 [*European Environmental Agency* (*EEA*), 2014]. Moreover, the eruption emitted volcanic SO_2 at a significantly higher rate than some of the most prolific continuously degassing volcanoes in the world like Kīlauea Volcano (Hawai`i) with SO_2 fluxes of between 2 kt/d and 8 kt/d on average [*Elias and Sutton*, 2012; *U.S. Geological Survey* (*USGS*), 2013] and Mount Etna (Italy) with an average SO_2 emission rate of 3.5 kt/d between 2005 and 2008 [*Salerno et al.*, 2009]. Overall, the 2014–2015 eruption at Holuhraun was the largest tropospheric volcanic sulfur pollution event since the 2000–2003 eruption of

Miyake-jima volcano in Japan [*Kazahaya et al.*, 2004] and the 1783–1784 C.E. Laki eruption in Iceland [*Thordarson et al.*, 1996; *Thordarson and Self*, 2003]. The latter is thought to have caused cooling of climate and environmental stress across Europe in the 1780s [e.g., *Thordarson and Self*, 2003; *Schmidt et al.*, 2010, 2011, 2012a]. Exposure to volcanic sulfur pollution has also been statistically linked to adverse effects on human health [e.g., *Longo et al.*, 2008, 2010; *Longo*, 2013].

Over the course of the 2014–2015 eruption at Holuhraun, air quality monitoring stations in the near field in Iceland recorded unprecedented levels of SO_2 concentrations at the surface [*Gíslason et al.*, 2015], often significantly exceeding the current 10 min mean air quality standard for SO_2 of 500 $\mu g/m^3$ set by the World Health Organization (WHO) to protect public health [*World Health Organization* (*WHO*), 2014]. Volcanic SO_2 from the eruption was also detected in the far field (i.e., at least 500 km from the eruption site) on a regular basis by satellite instruments from 1 September 2014 [*Support to Aviation Control Service*, 2014; *Ialongo et al.*, 2015], but a detailed analysis of these data sets has not yet been carried out.

Here we analyze surface air quality measurements across Northern Europe and satellite remote sensing data of volcanic SO_2 as well as model simulations using the United Kingdom Met Office's NAME model (Numerical Atmospheric-dispersion Modelling Environment). These data sets are used to investigate the degradation of air quality and the potential impacts on human health due to volcanic SO_2. We simulate the dispersion and chemical conversion of volcanic SO_2 from the eruption over the course of September 2014. Comparing the model simulations to surface measurements and satellite data enables both a detailed model evaluation and constraining the range and variability of the SO_2 source flux independent of ground-based measurements. We further investigate the sensitivity of simulated near-surface volcanic SO_2 concentrations to the uncertainties inherent in eruption source parameters (i.e., SO_2 flux and plume height) and model parameterizations (i.e., subgrid vertical diffusion and the boundary layer height). We conclude by discussing the implications for future flood lava eruptions in Iceland and for forecasting and monitoring volcanic SO_2 concentrations hundreds of kilometers away from a volcanic source using atmospheric models and satellite data.

2. Methods

2.1. Model Simulations and Comparison to Surface SO_2 Observations

In order to simulate long-range transport and air quality impacts of volcanic SO_2 emitted by the eruption, we use the Lagrangian dispersion model, NAME [*Jones et al.*, 2007]. NAME is also used for air quality modeling and forecasting and emergency response work such as predicting the dispersion of hazardous radiological, volcanic, chemical, or biological material [e.g., *Webster et al.*, 2006; *Derwent et al.*, 2007; *Redington et al.*, 2009; *Leadbetter and Hort*, 2011; *Leadbetter et al.*, 2012, 2015]. The London Volcanic Ash Advisory Centre uses NAME to operationally forecast volcanic ash dispersion [*Webster et al.*, 2012; *Witham et al.*, 2012]. Previously, NAME has been used to simulate SO_2 and sulfuric acid aerosol mass concentrations for the eruptions of Kasatochi in 2008, Sarychev in 2009, and Eyjafjallajökull in 2010 [*Heard et al.*, 2012; *Schmidt et al.*, 2014]. *Schmidt et al.* [2014] comprehensively evaluated the ability of NAME to predict the dispersion and the far-field concentrations of SO_2 for the 2010 Eyjafjallajökull eruption using a combination of satellite retrievals and in situ measurements. They found that for Eyjafjallajökull 2010 with plume heights up to 9 km, the model most frequently underpredicted vertical column densities of volcanic SO_2 by up to 3 Dobson units (DU) when compared to satellite retrievals. Furthermore, when compared to in situ aircraft observations, maximum SO_2 mixing ratios at specific locations and altitudes were not captured by the model simulations.

In this study, we perform a set of simulations using NAME (version 6.3) over the period 31 August to 30 September 2014 quantifying the sensitivity of the results to different assumptions about the eruption source parameters. We use four different SO_2 fluxes (20 kt/d, 40 kt/d, 60 kt/d, and 120 kt/d) and three different ranges of emission height (0–1500 m above ground level (agl), 1500–3000 m agl, and 4000–4500 m agl) emitted at 16.83°W, 64.87°N (Table 1). In the model, SO_2 is emitted as a continuous mass flux per second. Volcanic SO_2 is uniformly distributed in the vertical between the bottom and top height chosen for each simulation. A lack of continuous ground-based SO_2 flux measurements near the source region prevents the use of a more detailed time-varying flux. However, we are able to constrain credible ranges of the SO_2 fluxes based on our results using model simulations and interpreting satellite data. The SO2 fluxes we obtain are compared with

Table 1. Overview of Model Simulations and Normalized Mean Bias (NMB, in %) Comparing Simulated Sulfur Dioxide (SO_2) Vertical Column Densities (VCDs) to Satellite Retrievals From OMI and IASI[a]

			Normalized Mean Bias (%) OMI (IASI) Versus NAME SO_2 VCDs	
Run	SO_2 Emission (kt d^{-1})	Emission Altitude (m agl)	3–5 Sep 2014	23–28 Sep 2014
1	20	0–1500	−59.7 (−78.0)	−32.1 (−72.9)
2	20	1500–3000	−43.0 (−72.5)	−42.7 (−60.2)
3	20	4000–4500	−59.0 (−66.3)	−36.2 (−53.1)
4	40	0–1500	−31.5 (−52.9)	−20.5 (−41.0)
5	40	1500–3000	−8.3 (−42.9)	10.4 (−19.6)
6	40	4000–4500	−37.9 (−35.5)	−6.8 (−8.2)
7	60	0–1500	−12.6 (−26.9)	16.0 (−7.3)
8	60	1500–3000	9.1 (−13.2)	48.0 (20.5)
9	60	4000–4500	−22.0 (−6.4)	−40.5 (32.2)
10	120	0–1500	26.9 (47.0)	27.9 (85.6)
11	120	1500–3000	60.6 (51.4)	97.2 (103.4)
12	120	4000–4500	24.7 (65.7)	−0.2 (151.2)

[a]The NMB is calculated as follows: $NMB = 100\,\% \times \Sigma(M_i - O_i)/\Sigma O_i$ where M_i refers to the simulated SO_2 VCD and O_i to the satellite-derived SO_2 VCD.

initial estimates of the SO_2 flux obtained empirically by combining petrology [*Thordarson and Hartley*, 2015] and lava discharge rates [*Dürig et al*., 2015; *Höskuldsson et al*., 2015]. The model simulations are driven by meteorological fields from the Met Office Unified Model at 3-hourly temporal resolution with a horizontal resolution of about 0.234° longitude by 0.156° latitude and 59 vertical levels up to 30 km altitude [*Davies et al*., 2005]. In the boundary layer and free troposphere the vertical resolution of the meteorological fields is about 200 m. In addition, we carry out sensitivity simulations using operational meteorology from the European Centre for Medium-Range Weather Forecasts (ECMWF) at a resolution of 0.125° longitude by 0.125° latitude and 55 vertical levels up to 17 km. In all our simulations, we account for the chemical conversion of volcanic SO_2 in the gas phase via the reaction with the hydroxyl radical (OH), as well as conversion in the aqueous phase via the reaction with hydrogen peroxide (H_2O_2) and ozone (O_3) [*Redington et al*., 2009; *Schmidt et al*., 2014]. The OH radical, H_2O_2, and O_3 are modeled explicitly, accounting for oxidant depletion depending on SO_2 concentrations, with the latter two species being initialized at the start of the simulation from background fields provided by the STOCHEM chemical transport model [*Collins et al*., 1997; *Redington et al*., 2009]. Aqueous-phase oxidation occurs in model grid boxes where both liquid water and cloud fraction are nonzero, which are diagnosed from the Unified Model meteorological fields [*Redington et al*., 2009]. Removal of SO_2 and sulfuric acid aerosol particles occurs via dry and wet deposition [*Webster and Thomson*, 2011, 2014].

We present unratified but quality-checked hourly mean surface observations of SO_2 (Table 2 and Figure 2) from stations in Ireland (Irish Environmental Protection Agency), the United Kingdom (Department for

Table 2. Maximum SO_2 Mass Concentrations ($\mu g/m^3$) Measured at Surface Air Quality Monitoring Stations During September 2014 (See Also Figure 2)[a]

Country	Air Quality Monitoring Station	Longitude	Latitude	Date	Distance From Eruption Source (km)	Maximum Hourly Mean SO_2 Concentration ($\mu g/m^3$)
Iceland	Reyðarfjörður Hjallaleyra	14.24°W	65.03°N	13 Sep 2014 02:00	123	1509.3
Iceland	Reykjahlíð Grunnskóli	16.89°W	65.64°N	24 Sep 2014 17:00	86	1450.6
Ireland	Ennis	8.98°W	52.84°N	6 Sep 2014 17:00	1409	524.2
Ireland	Portlaoise	7.29°W	53.03°N	6 Sep 2014 16:00	1422	310.7
Ireland	Askeaton	8.95°W	52.63°N	6 Sep 2014 18:00	1432	451.6
Finland	Sammaltunturi	24.12°E	67.98°N	7 Sep 2014 22:00	1818	186.5
Scotland	Kirkwall	2.96°W	58.98°N	21 Sep 2014 08:00	974	322.9
Netherlands	Philippine-Stelleweg	3.74°E	51.29°N	22 Sep 2014 14:00	1916	82.4
England	Harwell	1.32°W	51.57°N	22 Sep 2014 15:00	1725	96.6
England	Wicken Fen	0.29°E	52.29°N	22 Sep 2014 14:00	1703	96.1
Austria	Masenberg	15.89°E	47.35°N	22 Sep 2014 13:00	2755	247.0

[a]For all stations listed, forward and backward trajectory analysis confirmed that the sampled air originated from the 2014–2015 eruption site at Holuhraun (see also Figure S1).

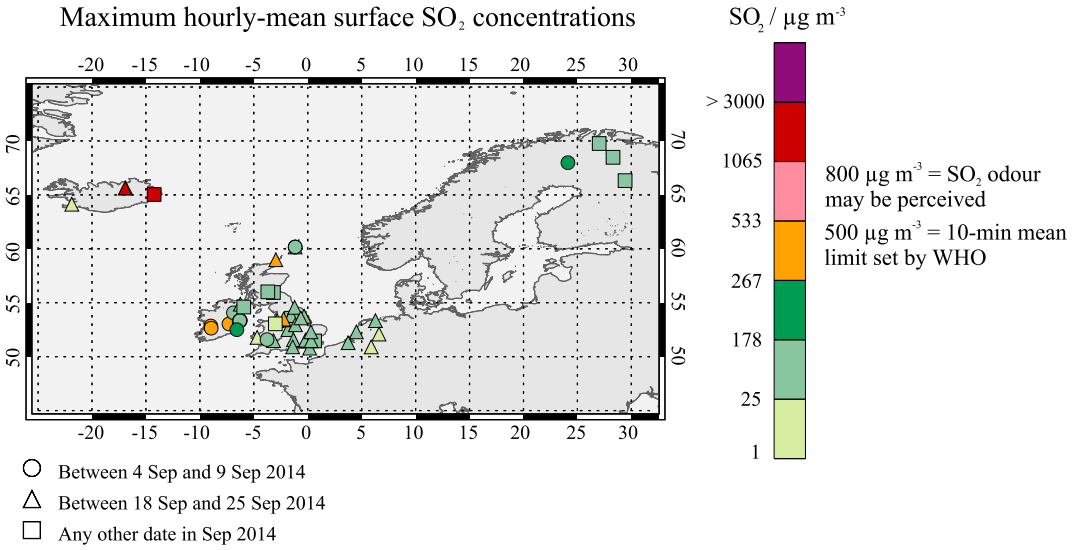

Figure 2. Maximum 1 h mean sulfur dioxide (SO_2) mass concentrations ($\mu g/m^3$) measured at the surface during September 2014 at air quality monitoring stations across Northern Europe (see also Table 2). Circles denote that these peak concentrations occurred between 4 and 9 September 2014, triangles denote the period 18–25 September 2014, and squares denote any other date in September 2014. The concentrations are color coded using the United Kingdom Department for Environment, Food and Rural Affairs (DEFRA) air quality index warning levels for 15 min mean SO_2 concentrations with green = low pollution levels, orange = moderate pollution levels, and pink = high pollution levels, and dark red and violet = very high and hazardous pollution levels [*Connolly et al.*, 2013]. Note that at times, in Iceland higher SO_2 mass concentrations have been measured after September 2014, which are not shown.

Environment, Food and Rural Affairs and Scottish Environment Protection Agency), Finland (Finnish Meteorological Institute), and the Netherlands (National Institute for Public Health and the Environment). These data are compared to model-simulated hourly mean output on a regular longitude-latitude grid of 0.5° by 0.5°. The air quality measurements are also used in conjunction with forward and backward trajectory analysis using NAME to constrain the SO_2 emission height at source for the most significant volcanic air pollution episodes recorded in Ireland on 6–7 September 2014 and in Scotland and other parts of the UK on 20–25 September 2014.

We also carry out sensitivity simulations in which we increase and decrease the free tropospheric vertical subgrid diffusion in NAME by a factor of 5. Inaccuracies in the strength of turbulence can result in an overestimation or underestimation of vertical spreading which, in turn, can lead to positional errors of the plume over long transport distances. In NAME, it is necessary to parameterize horizontal and vertical turbulent motions that are not resolved explicitly at the resolution of the input meteorology. This is achieved through the parameterization of subgrid diffusion, also referred to as eddy diffusivity. In the free troposphere, NAME uses a constant value for the horizontal and vertical subgrid diffusion, which is equal to the root-mean-square velocity multiplied by the timescale associated with the process. In detail, the vertical subgrid diffusion is given by

$$K_\omega = \alpha_\omega^2 \tau_\omega \quad (1)$$

where α_ω is the standard deviation of the vertical velocity in the free troposphere and τ_ω is the vertical Lagrangian timescale in the free troposphere. In NAME, α_ω is set to 0.1 m s^{-1}, and τ_ω is 100.0 s, resulting in a vertical eddy diffusivity K_ω of 1.0 m^2 s^{-1} [*Devenish et al.*, 2012a, and references therein]. Therefore, the standard deviation of the vertical distance that pollutants can be transported within 24 h is about 415 m. This distance is small compared to the vertical spread experienced due to resolved motions but not insignificant in light of pollutants experiencing different air masses and wind speeds. *Webster et al.* [2003] provide more detail about the turbulence parameterizations in NAME. *Dacre et al.* [2015] explored the sensitivity of ash cloud layer depth during the 2010 eruption of Eyjafjallajökull to assumptions made about the vertical subgrid diffusion. Using a space-time-varying vertical diffusivity scheme, they found that vertical diffusivity diagnosed based on clear air turbulence is generally lower than 1.0 m^2 s^{-1} with values

an order of magnitude higher occurring in a very small region only. Overall, they concluded that the space-time-varying vertical diffusivity scheme does not significantly outperform the scheme using a constant diffusivity in the vertical.

2.2. Satellite Retrievals and Comparison to Model Simulations

We further evaluate model performance by comparing to satellite retrievals of SO_2 for the period 31 August to 30 September 2014 from nadir measurements performed in the UV-visible by the Ozone Monitoring Instrument (OMI) on board Aura [*Levelt et al*., 2006] and in the thermal infrared by the Infrared Atmospheric Sounding Interferometer (IASI) on board MetOp-A and MetOp-B [*Clerbaux et al*., 2009]. Because of the partially overlapping orbits at high latitudes, OMI passes over Iceland about 3 times a day while IASI has six overpasses (day and night measurements). Vertical column densities of SO_2 (VCDs, expressed in Dobson units with $1\,\mathrm{DU} = 2.69 \times 10^{16}\,\mathrm{molecules\,cm^{-2}}$) are retrieved from OMI by applying Differential Optical Absorption Spectroscopy (DOAS) [*Platt and Stutz*, 2008] to the measured ultraviolet spectra. The algorithm is described in *Theys et al*. [2015] and also used in *Schmidt et al*. [2014] for the 2010 explosive eruption of Eyjafjallajökull. It makes use of a combination of three wavelength ranges (312 nm to 326 nm, 325 nm to 335 nm, and 360 nm to 390 nm). This allows for a low detection limit while avoiding saturation retrieval effects for high-magnitude SO_2 VCDs.

During the eruption, SO_2 resided in the lower troposphere; hence, the OMI retrieval is very sensitive to assumptions made about the plume height and to the presence of clouds (which can either mask or amplify the measured SO_2 signal depending on where the SO_2 is relative to the cloud). Moreover, measurements at high latitudes and high solar zenith angles are known to be unfavorable conditions for UV-visible tropospheric SO_2 retrievals. Therefore, the retrieval of SO_2 VCDs using OMI is challenging, and even using additional information on plume heights, the uncertainty on the VCDs is up to 50%. To estimate the uncertainty on the VCDs, we have calculated the errors associated with the different algorithmic steps (i.e., the retrieval of slant columns and the calculation of air mass factors [see also *Lee et al*., 2009]). For the slant column error, a multiplicative error of about ±25% is estimated based on test retrievals and accounts for uncertainties on the SO_2 absorption and spectral interferences in the DOAS fit. The nonmultiplicative error on the SO_2 slant columns is estimated to be small compared to the measured columns and has not been considered. Further uncertainty arises from the fact that some of the emitted SO_2 is not contributing to the SO_2 mass burden (i.e., SO_2 below the detection limit) that is, however, hard to quantify. For the air mass factor, an error of ±40% is estimated, which takes into account typical uncertainties due to the shape of the SO_2 profile, clouds, and surface reflectivity. Both error terms taken in quadrature result in a typical error on the SO_2 VCDs (and hence SO_2 mass burdens) of about ±50%, which is mostly systematic.

As described in *Theys et al*. [2015], the vertical measurement sensitivity functions (referred to as column operators), for which the effect of clouds on the retrievals is treated, are calculated for each OMI pixel. For this work, the VCDs are calculated using the medium column operators, corresponding to plume heights of about 7 km.

Compared to UV measurements, retrievals of lower tropospheric SO_2 plumes in the thermal infrared are notoriously difficult (mostly because of low thermal contrast and because of competing water vapor absorption) but also offer many advantages, especially for algorithms exploiting the full spectral information in the extended wavelength range and at high resolution. Besides being able to measure at night, IASI SO_2 retrievals are highly sensitive to the altitude of SO_2 [*Carboni et al*., 2012; *Clarisse et al*., 2014]. Here we use the algorithm of *Carboni et al*. [2012], which makes use of measurements of the SO_2 bands around 7.3 and 8.7 μm to jointly retrieve the SO_2 VCD and a proxy for the plume height under the assumption of a Gaussian vertical profile of SO_2. The IASI optimal estimation algorithm provides error estimates on the retrieved parameters for each pixel [*Carboni et al*., 2012]. The altitude of the SO_2 plume strongly modulates the retrieval error as the contrast between plume temperature and surface temperature is a critical factor. Typical uncertainties are 2 DU for a plume centered at 1.5 km and less than 1 DU for plumes above 3 km.

To compare model-simulated and satellite-retrieved VCDs of SO_2, the OMI column operators have been applied to the model-simulated 1-hourly mean SO_2 mass concentrations, which have been output at a vertical resolution of 200 m in the first 1000 m and 500 m between 1 km and 23 km. The column operators have been applied by taking each OMI pixel and finding the model profile that is coincident in both time (within

the model 1-hourly mean output resolution) and space (within a model grid box). The model profile is then interpolated to the OMI vertical retrieval grid, which results in a simulated VCD that is directly comparable to that derived using the satellite instruments.

In order to calculate metrics such as bias between the model outputs and the satellite retrievals, we gridded the satellite data onto the same regular 0.5° longitude by 0.5° latitude grid using all orbits between 0800 UTC and 1400 UTC for each day. To compare the model output to IASI, the IASI data are also gridded onto the same regular 0.5° longitude by 0.5° latitude grid as NAME using all orbits between 0800 UTC and 1500 UTC for each day. For NAME and also OMI and IASI, we calculated an average VCD in the case of overlapping plumes or orbits.

To derive the SO_2 mass burdens (i.e., the mass of SO_2 in the atmosphere at a given time) for each OMI orbit, we use IASI-derived plume heights, which enable us to directly compare the burdens derived from the two instruments. For the OMI retrieval we also account for the effects of clouds below the plume through the air mass factor calculation as described in *Theys et al*. [2015]. We compare the model-simulated burden calculated over the area 60°W–40°E and 75°N–45°N to those retrieved by OMI and IASI over the same area and average overlapping pixels in order to minimize double counting of SO_2 mass. The retrievals for both instruments are sensitive to the occurrence of clouds above the volcanic plume, which cannot easily be accounted for in contrast to the occurrence of clouds below the plume. Clouds above the volcanic plumes result in an underestimation of the SO_2 VCDs. The uncertainty on the OMI-derived mass burden is ±50% as described above. The uncertainty on the IASI burdens ranges from ±16% to ±75%. This uncertainty on the IASI burden is derived based on the optimal estimation algorithm described in *Carboni et al*. [2012], with error estimates corresponding to the sum of the errors estimated for pixels that have been identified as part of the volcanic SO_2 plume [*Walker et al*., 2011, 2012]. Small errors on the IASI SO_2 burden reflect the fact that the total number of pixels identified as SO_2 plume is low. In detail, the error budget for every pixel is derived from an error covariance matrix that is based on the SO_2-free climatology of the differences between the IASI and forward modeled spectra and includes instrumental errors, forward model errors (i.e., imperfect radiative transfer), errors in meteorological fields, and all the errors due to the lack of knowledge of the parameters that affect the radiance such as the imperfect representation of gas absorption (both profile and spectroscopy) and the presence of a cloud layer below the volcanic plume.

3. Results and Discussion

3.1. Long-Range Transport of Volcanic SO_2

In the NAME model, volcanic SO_2 from the eruption is dispersed about 3000 km from the source in Iceland despite the relatively low SO_2 emission altitudes of up to 4500 m agl. Our findings are corroborated by high hourly mean surface SO_2 concentrations of 247 $\mu g/m^3$ measured at an air quality monitoring station in Austria (Table 2) on 22 September 2014, about 2750 km away from the source [*Umweltbundesamt*, 2014; *Zentralanstalt für Meteorologie und Geodynamik*, 2014]. Pollutant transport from Iceland into Northern Europe during September 2014 was associated mainly with a series of anticyclones. In early September an anticyclone tracked slowly eastward across the United Kingdom and Scandinavia producing northerly winds that transported SO_2 from Iceland to Ireland on 3–6 September 2014 and then westerly winds, which transported SO_2 from Iceland to northern Finland (Figure S2 in the supporting information). An anticyclone located over the United Kingdom on 21–22 September coalesced with an anticyclone in the mid-Atlantic forming a ridge of high pressure over the United Kingdom. This anticyclone and the subsequent ridge of high pressure were associated with northwesterly winds, which transported SO_2 across from Iceland to the United Kingdom on 20–21 September 2014 and into the Netherlands by 22 September 2014 (Figure S2).

Long-range transport of volcanic gases and aerosol particles from nonexplosive volcanic eruptions has also been reported elsewhere [e.g., *Schmidt et al*., 2010, 2012b], but direct observations in the far field remain sparse, particularly in Europe. In 2010, nucleation of sulfuric acid aerosol particles in the far-field Eyjafjallajökull volcanic plume was, for the first time, observed at the high-altitude station of Puy-de-Dôme in central France [*Boulon et al*., 2011]. Tropospheric pollutant transport from the 2014–2015 eruption at Holuhraun can also be compared to other continuously degassing volcanoes around the world. For instance, volcanic pollutants in the troposphere from the 1983 to present eruption of Kīlauea Volcano on Hawai`i Island

[*USGS*, 2013] have been detected by satellites at distances greater than 1000 km from the volcano [e.g., *Yuan et al*., 2011]. Similarly, *Tu et al*. [2004] presented airborne SO_2 measurements from the September 2000 to December 2003 eruption of Miyake-jima volcano on Miyake Island southeast of Honshū in Japan, showing that sulfur can be detected in the troposphere of the central Pacific about 4000 km away from the source.

3.2. SO_2 Vertical Column Densities and Plume Heights

Although using satellites to retrieve SO_2 VCDs for high-latitude, tropospheric volcanic plumes is difficult and subject to large uncertainties [e.g., *Ialongo et al*., 2015], we show here that during September 2014 both IASI and OMI successfully detected SO_2 from the 2014–2015 eruption at Holuhraun (Figure 3). In general, the locations of the satellite-detected plumes are in good agreement with those locations at which air quality monitoring stations detected high surface SO_2 concentrations during September 2014 (section 3.4). However, peak SO_2 VCDs detected in the far field on 5 and 21 September 2014 differ significantly between the two satellite instruments, by up to an order of magnitude. We interpret these deviations as being due to differences in spatial resolution and more importantly on vertical measurement sensitivity and assumptions made in the retrieval (e.g., for the OMI VCDs we assume a SO_2 height of 7 km while IASI height retrievals often indicate a much lower plume). In section 3.3 we demonstrate that OMI and IASI are in reality fairly consistent when the SO_2 mass burdens are compared (to avoid differences due to spatial resolution) and when using the plume height derived from IASI to constrain the OMI SO_2 mass burden calculations.

For the period 5–6 September 2014, we find good agreement between the SO_2 VCDs retrieved by OMI and IASI and those simulated using NAME for a simulation in which 60 kt/d have been emitted into altitudes between 4000 and 4500 m agl. (Table 1 and Figure 3). For this model run, peak-simulated SO_2 VCDs near Ireland on 6 September 2014 reach 17 DU (sampled at OMI overpass times and with the OMI column operators applied to the model output) compared to OMI VCDs of 11 DU, and 45 DU (sampled at IASI overpass times) compared to IASI VCDs of 45 DU. Table 1 lists the normalized mean bias (NMB) for all simulations over this period. An emission altitude of 4000–4500 m agl during early September 2014 is also confirmed by ground-based and airborne observations of the plume height in Iceland, as well as forward and backward trajectory analysis, using the locations of surface SO_2 measurements in Ireland and Scotland (Figure S1). Using IASI, we find near-source heights of up to 2700 m above sea level (asl) where the highest SO_2 mass concentrations are detected in the vertical column and mean plume heights of up to 3700 m asl on 3 September 2014 (Table S1). On 21 September 2014 there are large discrepancies in the simulated location of the plume compared to the satellites. Both IASI and OMI detect SO_2 VCDs greater than 2 DU near the Dutch coast, whereas in simulations emitting SO_2 up to 1500 m altitude the plume does not reach that far south (Figure 3). However, emitting between 40 kt/d and 60 kt/d between 1500–3000 m agl and 4000–4500 m agl altitude resolves this discrepancy although this then results in simulated SO_2 VCDs between Iceland and the United Kingdom being greater in NAME compared to the satellite data (Figure 3). Backward trajectory analysis combined with surface observations in Northern Scotland also corroborates an increase in plume heights to 3000 m asl on 20 September 2014 (Figure S1). Plume heights of 3100 m asl are further supported by IASI for 19 September 2014 (Table S1).

3.3. SO_2 Mass Burden, Fluxes, and Lifetimes

Figure 4 shows a time series of SO_2 mass burdens for September 2014 derived using OMI, IASI, and NAME totaled over the area 60°W–40°E and 75°N–45°N. Although there are substantial uncertainties on the mass burdens derived using OMI and IASI, we show here that the eruption contributed significantly to the total mass of SO_2 in the atmosphere. For September 2014, we calculate an average daily SO_2 mass burden of 99 ± 49 kt of SO_2 from OMI and 61 ± 18 kt of SO_2 based on IASI morning orbits. Averaging the IASI morning and afternoon orbits, the average daily SO_2 mass burden is 55 ± 17 kt of SO_2 for September 2014 (Table S2). For comparison, the typical annual mean burden in the same geographical region was about 120 kt of SO_2 in the 1970s when SO_2 emissions in Europe peaked and 20 kt of SO_2 during 2009 (based on aerosol-climate model simulations by *Turnock et al*. [2015]). In these simulations, the September mean SO_2 burden averaged for the years 2007 to 2009 over the area 60°W–40°E and 75°N–45°N was 16.9 kt of SO_2, indicating that the atmospheric burden over Europe at least doubled due to eruption in September 2014.

Compared to the satellite burdens, our model simulations suggest SO_2 fluxes of 120 kt/d during the initial phases of the eruption, which is in good agreement with initial estimates from ground-based optical remote

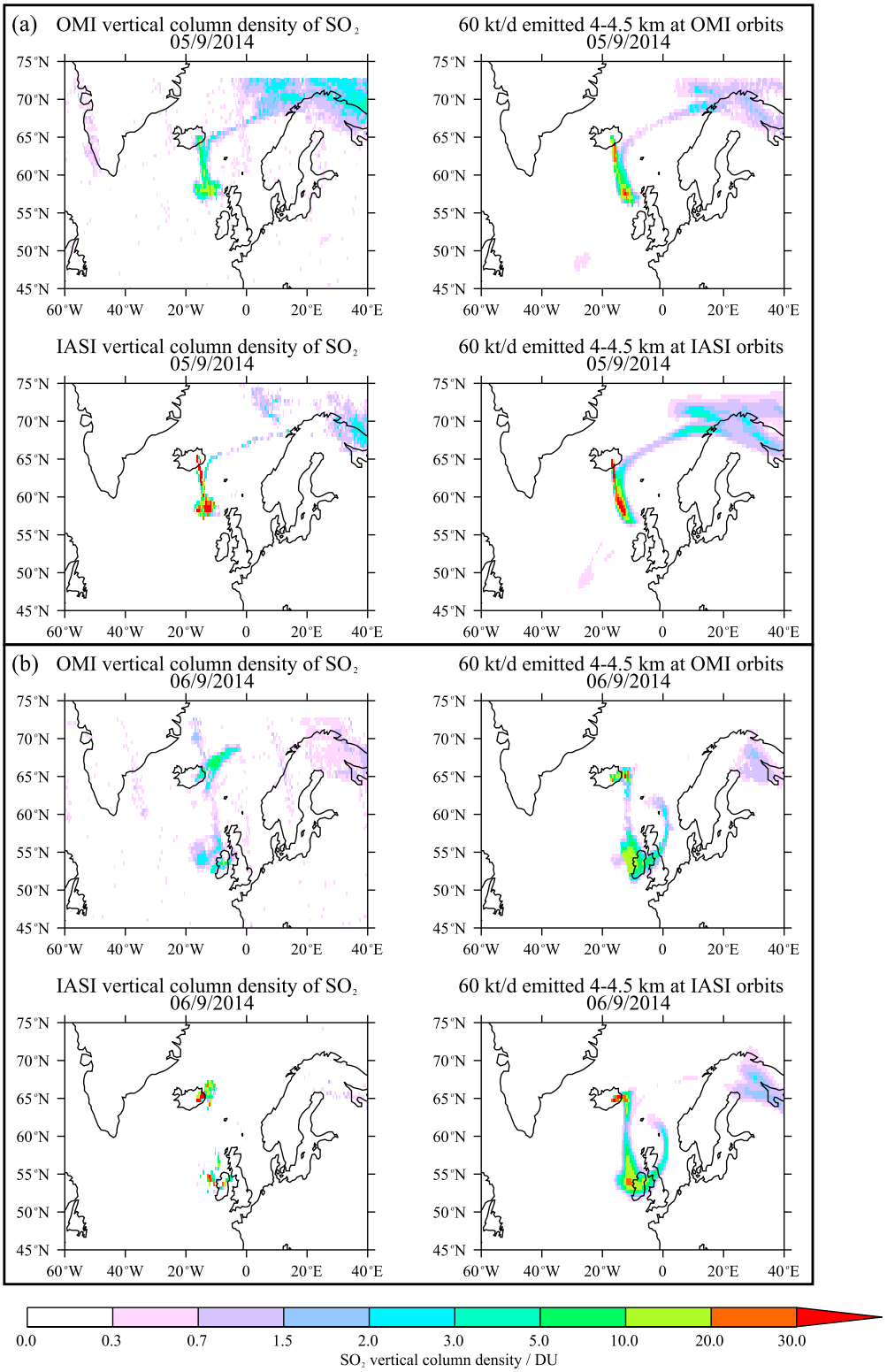

Figure 3. Comparison of satellite-retrieved and satellite-simulated SO_2 vertical column densities (VCDs) for 5–6 and 20–21 September 2014. For the comparison of the model simulations to the Ozone Monitoring Instrument (OMI) the model output was sampled at OMI overpasses and the column operator was applied, and for the comparison to the Infrared Atmospheric Sounding Interferometer (IASI) the model was sampled at IASI overpasses between 08:00 UTC and 15:00 UTC. Both the OMI and IASI data have been gridded onto the same regular 0.5° by 0.5° longitude-latitude grid as the model simulations.

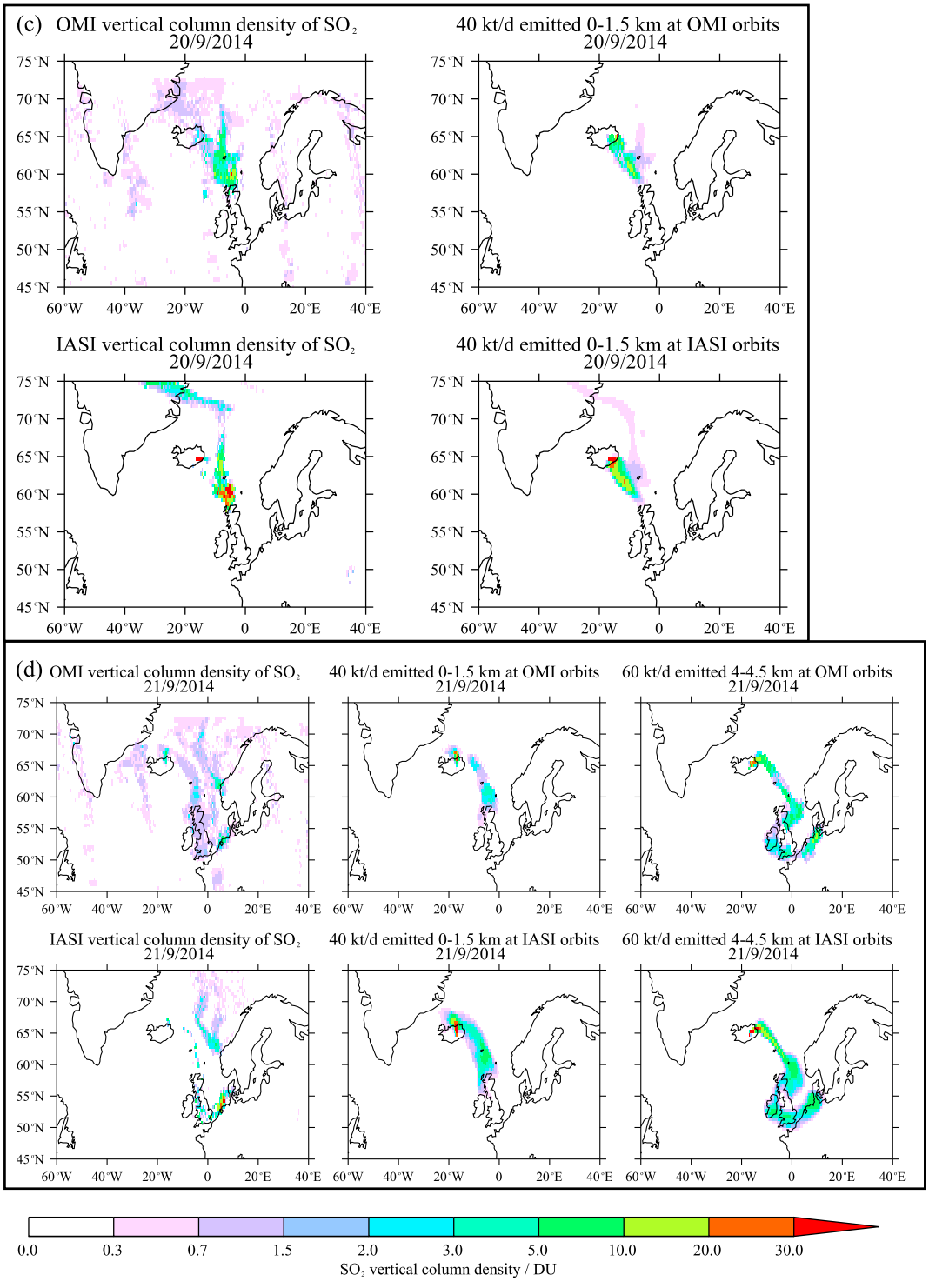

Figure 3. (continued)

sensing [*IMO*, 2014] and at the lower end of empirical estimates combining lava discharge rates and petrology [*Thordarson and Hartley*, 2015]. For 6–22 September 2014 the model to satellite comparison suggests emission rates of 20–60 kt/d followed by a period of higher emission rates of 60–120 kt/d until the end of September 2014. For mid-September 2014, an overall reduction in the SO_2 emission rate and plume height is supported by both a decline in lava discharge rates to about 160 m^3/s [*Höskuldsson et al.*, 2015] and observations of the

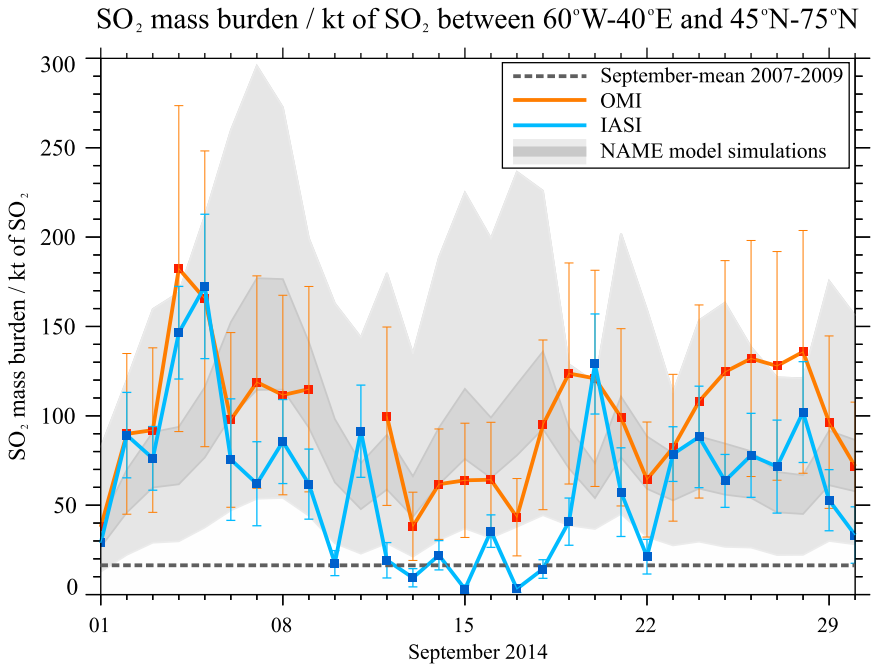

Figure 4. Comparison of satellite-derived and satellite-simulated SO_2 mass burdens in kilotons (kt) for September 2014 totaled between 60°W to 40°E and 45°N and 75°N (i.e., the same domain as used for Figure 3). The mass burdens derived from the Ozone Monitoring Instrument (OMI) are shown in orange, using plume heights derived from the Infrared Atmospheric Sounding Interferometer (IASI). The IASI-derived mass burdens are shown in blue. The lower bound of the light gray shading shows the mass burden from a simulation emitting 20 kt/d of SO_2 into 1500–3000 m agl altitude, and the upper bound shows the mass burden from a simulation emitting 120 kt/d of SO_2 into 1500–3000 m agl altitude. The upper and lower bounds of the dark gray shading refer to model simulations in which 40 kt/d and 60 kt/d of SO_2 have been emitted into 1500–3000 m agl altitude. The dark gray dashed line shows the September mean SO_2 mass burden averaged for the years 2007 to 2009 based on model simulations by *Turnock et al.* [2015]. In addition, Table S2 in the supporting information lists the daily mean mass burdens for all simulations listed in Table 1.

plume height in Iceland as well as those retrieved using IASI (Table S1). Empirical estimates of the SO_2 flux for lava discharge rates of 160 m^3/s would, however, suggest SO_2 fluxes between 50 kt/d and 110 kt/d, implying that for mid-September our method results in flux estimates that are below the lower end of the empirical estimates [*Thordarson and Hartley*, 2015].

For OMI, the uncertainties on SO_2 mass burdens are ±50% as detailed in section 2.2. For IASI, uncertainties on the daily mass burdens are up to ±75% (section 2.2 and Table S2). It is also apparent in Figure 4 that on 13 and 17 September 2014 the gridded SO_2 mass burden derived from IASI decreases to very low values (<5 kt of SO_2) between periods of higher mass burdens, which cannot be solely explained by physical or chemical processes at the source or in the atmosphere but rather by the low sensitivity of IASI to very low altitude plumes (because of the low thermal contrast). Although there are differences in the SO_2 VCDs derived using IASI and OMI (section 3.1), we find fair agreement between the instruments with error bars overlapping on about two thirds of the days when deriving the SO_2 mass burdens shown in Figure 4 using the IASI height information as a prior for the OMI retrieval. The IASI retrieval used here could be exploited to derive both the daily SO_2 mass burdens and plume heights over the entire course of the eruption, which is not possible with an ultraviolet sensor like OMI due to the lack of sunlight at high northern latitudes during boreal winter.

The simulated volcanic SO_2 mass burdens vary significantly on a daily basis (gray lines and shading in Figure 4). Given that in our model, volcanic SO_2 is the only source and that we are using constant volcanic emission fluxes, the variation in the SO_2 burdens must be a result of short-term variations in the chemical loss and/or dry deposition rates of volcanic SO_2. Therefore, the setup of our model allows us to diagnose an effective steady state mean SO_2 lifetime for September 2014, by dividing the simulated daily burden over the whole model domain (Table S3) by the emission rate for each simulation. The derived volcanic SO_2 lifetime is 2.0 days ($\sigma = 0.8$ days; range of 0.4 days to 4.0 days; Table S4). Model simulations and satellite observations

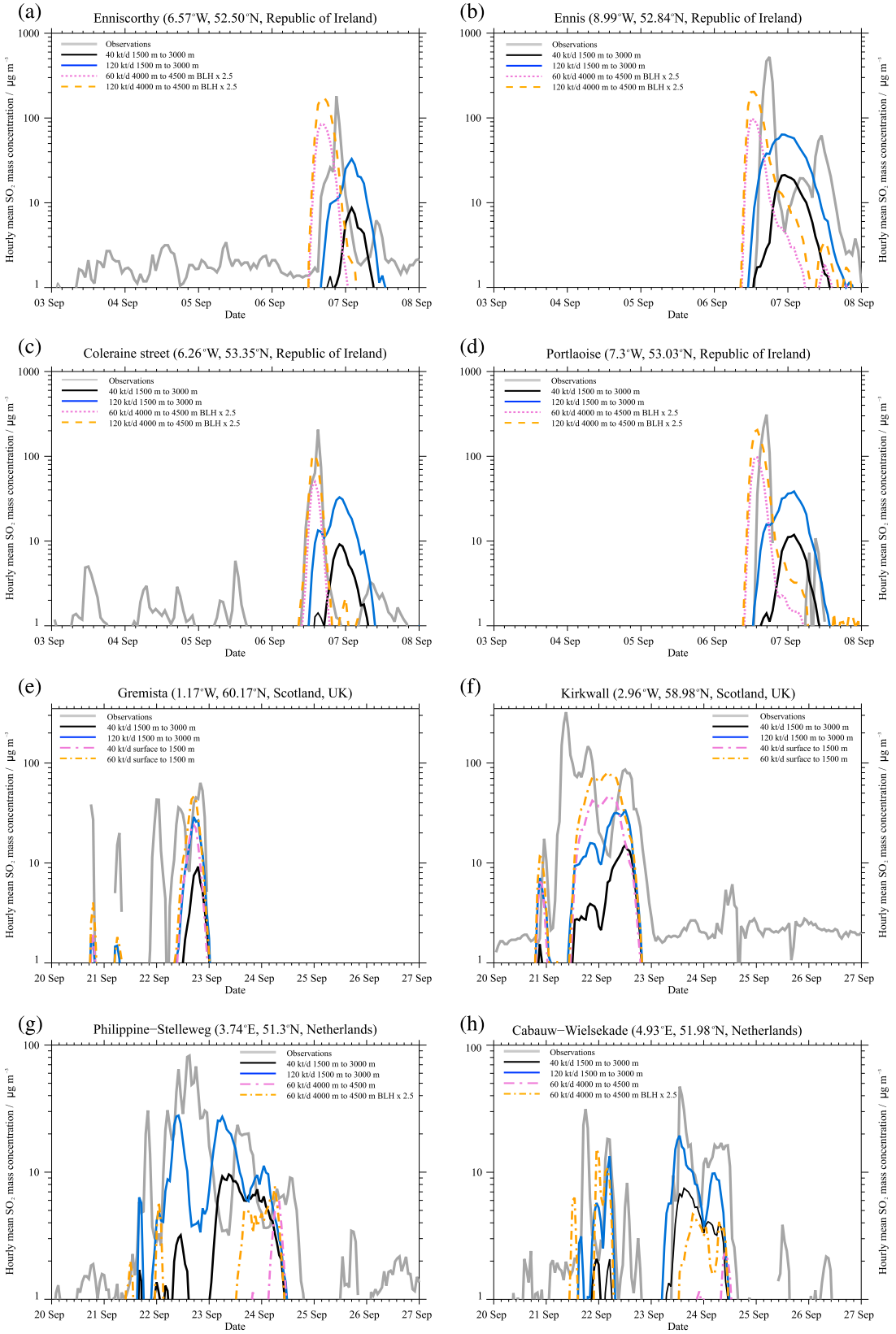
(a)
Enniscorthy (6.57°W, 52.50°N, Republic of Ireland)
(b)
Ennis (8.99°W, 52.84°N, Republic of Ireland)
(c)
Coleraine street (6.26°W, 53.35°N, Republic of Ireland)
(d)
Portlaoise (7.3°W, 53.03°N, Republic of Ireland)
(e)
Gremista (1.17°W, 60.17°N, Scotland, UK)
(f)
Kirkwall (2.96°W, 58.98°N, Scotland, UK)
(g)
Philippine−Stelleweg (3.74°E, 51.3°N, Netherlands)
(h)
Cabauw−Wielsekade (4.93°E, 51.98°N, Netherlands)
Observations
40 kt/d 1500 m to 3000 m
120 kt/d 1500 m to 3000 m
60 kt/d 4000 m to 4500 m BLH x 2.5
120 kt/d 4000 m to 4500 m BLH x 2.5
40 kt/d surface to 1500 m
60 kt/d surface to 1500 m
60 kt/d 4000 m to 4500 m
Hourly mean SO2 mass concentration / µg m-3
Date
03 Sep
04 Sep
05 Sep
06 Sep
07 Sep
08 Sep
20 Sep
21 Sep
22 Sep
23 Sep
24 Sep
25 Sep
26 Sep
27 Sep

Figure 5

of SO_2 from anthropogenic sources and continuously degassing volcanoes show that SO_2 emitted into the boundary layer and free troposphere typically has a lifetime of 1 to 3 days [e.g., *Stevenson et al*., 2003; *Lee et al*., 2011; *Schmidt et al*., 2012b; *Carn et al*., 2013; *McCormick et al*., 2014]. For steady state degassing under cloud-free conditions and a stable wind regime, *Beirle et al*. [2014] showed that emission rates and lifetimes can be derived simultaneously (without the need for a chemical transport model) using satellite data together with reanalyzed meteorology. However, our results show that the SO_2 lifetime can vary significantly on a daily basis; hence, calculating SO_2 mass fluxes from satellite-derived mass burdens using a constant SO_2 lifetime may not be entirely appropriate for continuously degassing volcanoes.

Based on the derived SO_2 fluxes, we calculate that the eruption emitted a total of 2.0 ± 0.6 Tg of SO_2 during September 2014, which is in good agreement with ground-based remote sensing [*Gíslason et al*., 2015] and petrological estimates [*Thordarson and Hartley*, 2015]. For context, the 2000–2003 Miyake-jima eruption was the biggest tropospheric volcanic pollution event at the time. The eruption emitted a total of 18 Tg of SO_2 with a maximum daily SO_2 flux of 54 kt/d measured in December 2000 [*Kazahaya et al*., 2004], which is about half the maximum daily SO_2 flux estimated for the 2014–2015 eruption at Holuhraun [*Thordarson and Hartley*, 2015]. Over the course of 6 months the 2014–2015 eruption at Holuhraun emitted at total of 11 ± 5 Tg of SO_2 [*Gíslason et al*., 2015; *Thordarson and Hartley*, 2015], which is about a factor of 2 greater than the total SO_2 mass emitted by Miyake-jima during its first 6 months of activity [*Kazahaya et al*., 2004].

3.4. Surface Air Quality Impacts

During September 2014, air quality measurements of SO_2 across Northern Europe (Figures 2 and 5) showed an increase in surface SO_2 concentrations compared to typical background concentrations in Europe, which were less than 6 $\mu g/m^3$ on average in 2010 [*EEA*, 2013]. Two significant volcanic pollution episodes were observed, one on 4–8 September 2014 when one 1-hourly mean surface observation in Ennis in the Republic of Ireland reached ~524 $\mu g/m^3$ and a second on 20–25 September 2014 when observations in Scotland reached ~320 $\mu g/m^3$ (Table 2 and Figures 2 and 5). In Finland peak hourly mean surface SO_2 concentrations of ~180 $\mu g/m^3$ were measured at Sammaltunturi during the night of 7–8 September 2014 [*Ialongo et al*., 2015]. In the Netherlands and England, peak hourly mean surface SO_2 concentrations of ~82 $\mu g/m^3$ and ~96 $\mu g/m^3$ were measured on 22 September 2014. For context, the last time hourly mean surface SO_2 mass concentrations of ~400 $\mu g/m^3$ were measured in Europe was in 1990 (data from http://ebas.nilu.no/).

Figure 5 compares observed and simulated SO_2 surface concentrations at selected stations in the Republic of Ireland, Scotland, and the Netherlands for the periods 3–8 and 20–27 September 2014. Even for the high emission rate of 120 kt/d, the model simulations (Table 1) underpredict surface SO_2 mass concentrations at stations in Ireland by up to a factor of 8. For 6–7 September 2014 simulated peak surface concentrations slightly lag behind those measured in Ireland by about 4 h (solid lines in Figure 5). For 21 September 2014 peak-observed surface SO_2 concentrations of about 320 $\mu g/m^3$ in Kirkwall (Scotland) are a factor of 4 greater than the simulation emitting 60 kt/d between the surface and 1500 m agl (Figure 5).

In order to understand the discrepancy of simulated and observed peak surface SO_2 concentrations in the Republic of Ireland, we show vertical cross sections at 17:00–18:00 UTC on 6 September 2014 along 52.8°N for simulations emitting 60 kt/d and 120 kt/d of SO_2 into 4000–4500 m agl altitude (Figure 6). It is apparent that in the model simulations, SO_2 concentrations of comparable magnitude to those measured at the surface occur above the boundary layer at altitudes >1500 m agl. Peak SO_2 concentrations of ~315 $\mu g/m^3$ for the 60 kt/d and ~633 $\mu g/m^3$ for the 120 kt/d simulation occur to the east of the Irish monitoring site at Ennis. In this case, these relatively small errors in the vertical and horizontal positioning of the dispersed volcanic plume in the far field result in a lack of pollutant entrainment from the free troposphere into the boundary layer because concentrations do not reach the top of the boundary layer. We find little difference in the position and concentration of the volcanic SO_2 plume for the period 3–8 September 2014 when either

Figure 5. Time series of observed (solid gray lines) and simulated surface SO_2 mass concentrations ($\mu g/m^3$) for selected air quality monitoring sites in the (a–d) Republic of Ireland, (e and f) Scotland, and (g and h) the Netherlands. The solid black lines show output from a simulation in which 40 kt/d of SO_2 have been emitted into altitudes between 1500 m and 3000 m above ground level, and the solid blue lines refer to a simulation in which 120 kt/d have been emitted into 1500 m and 3000 m altitude above ground level. The pink and orange lines refer to specific sensitivity simulations as indicated in each plot with BLH × 2.5 referring to an increase in the boundary layer height by a factor of 2.5 in the model.

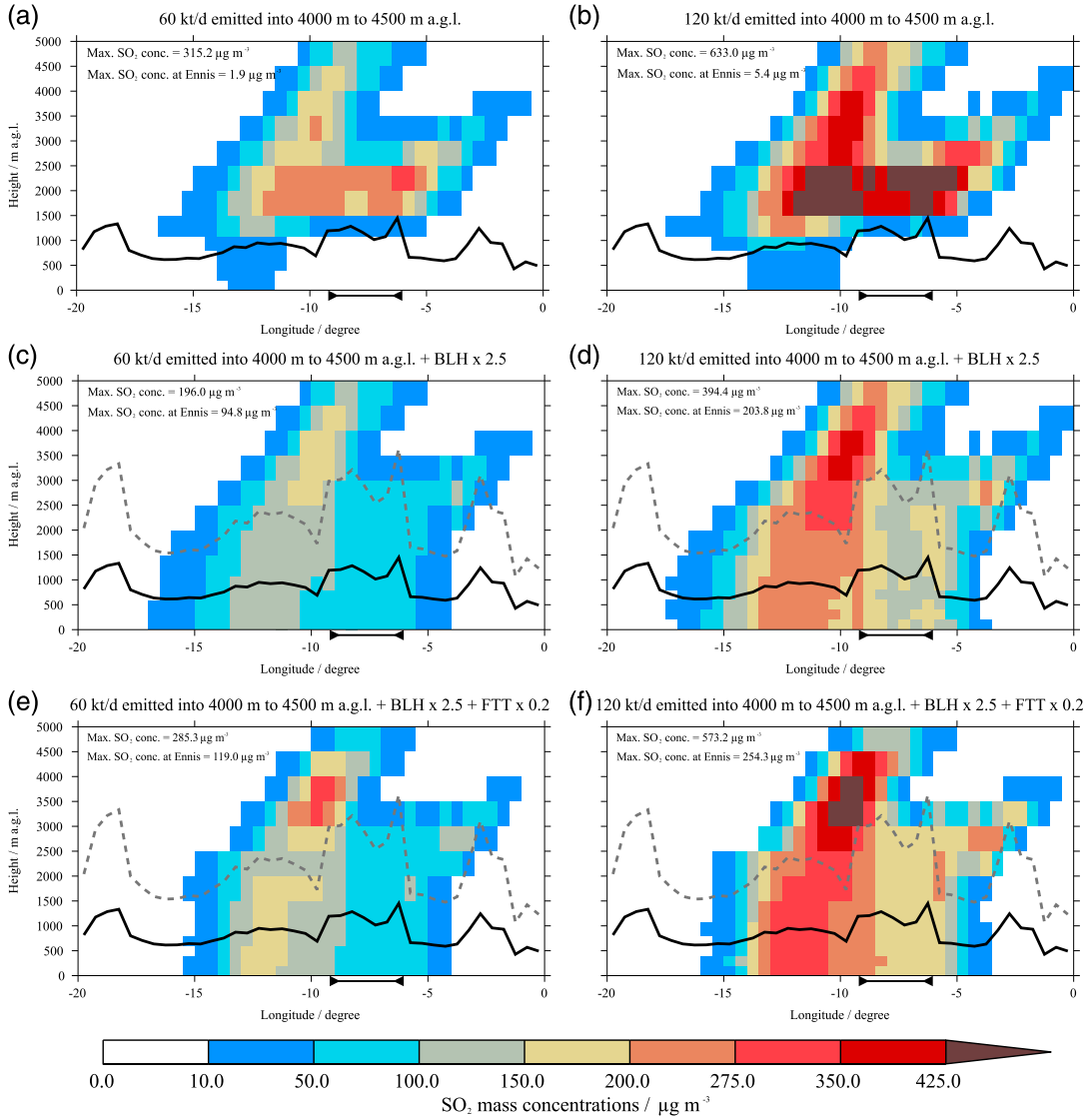

Figure 6. Vertical cross sections of SO_2 mass concentrations (µg/m^3) at 17:00–18:00 UTC on 6 September 2014 along 52.8°N (the latitude of the Irish observation station, Ennis) for (a and b) simulations emitting 60 kt/d and 120 kt/d of SO_2 into 4000–4500 m agl altitude. The black line underneath the *x* axis shows the longitude range for all monitoring stations in the Republic of Ireland. The boundary layer height (BLH in meters above ground level, m agl) from the Unified Model is shown as solid black line. (c and d) The same simulations as in Figures 6a and 6b, but in the model the boundary layer height was increased by a factor of 2.5 as shown by the dashed gray line. (e and f) The same simulations as in Figures 6a and 6b, but in the model the boundary layer height has been increased by a factor of 2.5 and the vertical subgrid diffusion or free tropospheric turbulence (FTT) decreased by a factor of 5.

increasing the horizontal resolution to 0.25° by 0.25° or using ECMWF analysis as opposed to using meteorological fields from the Unified Model (not shown).

We carry out sensitivity simulations in order to understand whether either the boundary layer height diagnosed in the model is incorrect compared to reality or whether the vigor of subgrid diffusion can explain the positional errors of the dispersed plume apparent in Figure 6. First, by increasing the boundary layer height in the model by a factor of 2.5, we find that simulated peak surface concentrations at Ennis reach about 95 µg/m^3 and about 204 µg/m^3 for the 60 kt/d and 120 kt/d simulations (Figures 6c, 6d, and 5b, dashed lines). We also find that the timing of the peak is in much closer agreement to the observations in these simulations.

A radiosonde observation from the coastal location of Valentia in the Republic of Ireland on 6 September 2014 at 12:00 UTC (Figure S3) shows a very shallow unstable layer within 100 m (1000 hPa) of the surface,

moist stable stratified air between 100 m and 1500 m (1000–830 hPa) and dry stable stratified air above. The sharp gradient in the modeled plume occurs at 1500 m (850 hPa), which coincides almost exactly with the change between the moist and dry air in the tephigram. This change could well illustrate the interface between two air masses of different origin. The boundary layer height from the Unified Model is at 900 m (900 hPa) at the time and location of the tephigram, which is in the middle of the stable stratified moist air mass and thus appears unrealistic. Observations at Valentia are only available at 00:00 UTC and 12:00 UTC, so it is not possible to show how the observed vertical profile developed between 12:00 UTC and 18:00 UTC. It is, however, unlikely that at either the coastal location of the tephigram or farther inland, a well-mixed boundary layer grew to the altitudes of 2500 m or more that were necessary to bring pollutants down to the surface in the model (typical regional values for September are 1000–1500 m). For this reason, errors in the model boundary layer height alone cannot fully explain the bias in the simulations. The fact that simulated surface SO_2 concentrations increased in the simulations where the pollutants intercept the top of the boundary layer, however, gives confidence in the model's boundary layer entrainment parameterization.

Second, we increased and decreased the vertical subgrid diffusion (see section 2 for details). None of these sensitivity simulations give a markedly better agreement with the surface observations on 6 September 2014 (Figure S4). Decreasing the vertical subgrid diffusion results in thinner plumes with higher concentrations that are, however, still residing above the boundary layer. In contrast, increasing the vertical subgrid diffusion results in a deeper plume of lower SO_2 mass concentrations, which descends further reaching the model's boundary layer. The resulting entrainment into the boundary layer leads to very small increases in surface SO_2 concentrations for both the 60 kt/d and 120 kt/d simulations. Out of all of the sensitivity simulations, we find best agreement with the surface observations at Ennis for the 120 kt/d simulation in which the vertical subgrid diffusion is decreased by a factor of 5 and the boundary layer height is increased by a factor of 2.5 (Figure 6f).

Figure 6 also shows that there is a very sharp gradient in pollutant concentration at an altitude of 1500 m, which may suggest that the chosen vertical output resolution of NAME (500 m) and/or that of the meteorological fields (200 m) used to drive the model are too coarse around the top of the boundary layer to adequately represent the fine balance between the altitude of the plume and the extent of boundary layer mixing. Overall, our model simulations demonstrate that relatively small errors in the height of the boundary layer top and the vertical and horizontal position of the dispersed plume in the far field can lead to large errors in surface concentrations at specific locations. Using atmospheric dispersion models for quantitative prediction of surface SO_2 concentrations at specific locations is subject to uncertainties in the meteorological fields, vertical resolution, pollutant removal rates (i.e., via chemical conversion of SO_2 to sulfate aerosol and/or dry deposition of SO_2), subgrid turbulence parameterizations, and the eruption source terms such as the emission altitude at a high temporal resolution. These issues are inherent to all dispersion problems independent of the pollutant considered. For instance, *Devenish et al*. [2012a], *Webster et al*. [2012], and *Dacre et al*. [2015] showed that simulations of volcanic ash concentrations and the thickness of volcanic ash plumes for the 2010 Eyjafjallajökull eruption are affected by positional errors and the vigor of both small-scale horizontal and vertical turbulence. Similarly, *Kristiansen et al*. [2012] performed multimodel ensemble simulations of volcanic ash transport for the 2010 Eyjafjallajökull eruption showing that simulated peak ash concentrations are often lower than observed and subject to positional errors.

3.5. Health Risks Due To Exposure to Volcanic SO_2

Both short-term and long-term exposure to air pollutants such as SO_2 and particulate matter can cause adverse health effects [e.g., *Rall*, 1974; *Pope et al*., 2002; *Hansell and Oppenheimer*, 2004; *Cohen et al*., 2005; *Pope and Dockery*, 2006; *Longo et al*., 2008; *WHO*, 2008; *Brook et al*., 2010; *Longo et al*., 2010; *Longo*, 2013]. For SO_2, the WHO sets a 10 min mean air quality standard of 500 $\mu g/m^3$ to protect human health [*WHO*, 2014]. The Clean Air for Europe directive states that if surface SO_2 mass concentrations exceed 500 $\mu g/m^3$ for more than three consecutive hours, the public must be notified [*EEA*, 2013]. During the 2014–2015 eruption at Holuhraun, far-field SO_2 mass concentrations peaked at ~524 $\mu g/m^3$ (Table 2), exceeding the WHO air quality standard for only 1 h at 17:00–18:00 on 6 September 2014 in Ennis in the Republic of Ireland. In Iceland, hourly mean surface SO_2 concentrations exceeded 350 $\mu g/m^3$ for more than 100 h in total (over the course of the entire eruption) and represented the highest concentrations ever recorded since measurements began [*Gíslason et al*., 2015]. Peak hourly mean concentrations of about 3000 $\mu g/m^3$ have been

measured in the southeast of Iceland at a station in Höfn (~100 km from eruption site) on 11 January 2015, and the 350 $\mu g/m^3$ threshold was exceeded for 124 h in total with a maximum of 16 consecutive hours exceeding this threshold since the beginning of the measurements at this station on 28 October 2014. Using hand-held SO_2 sensors, significantly higher peak SO_2 mass concentrations of about 20,000 $\mu g/m^3$ were measured in the south of Iceland. In contrast, the observations shown in Figure 5 (gray lines) show that for this eruption the volcanic pollution events in the far field were much shorter lived and concentrations were lower with exceedances of hourly mean SO_2 concentrations of 100 $\mu g/m^3$ lasting less than six consecutive hours.

In the United Kingdom, 15 min mean surface SO_2 concentrations of 266 $\mu g/m^3$ or greater are considered "moderate pollution" by the Department for Environment, Food and Rural Affairs (DEFRA) and there are specific recommendations associated with these pollution levels to protect public health [*Connolly et al*., 2013]. Likewise, SO_2 concentrations greater than 533 $\mu g/m^3$ and 1065 $\mu g/m^3$ are considered "high" and "very high" pollution by DEFRA. Based on hourly boundary layer mean output from our simulations, we calculate a maximum number of 11 consecutive hours above the SO_2 threshold of 266 $\mu g/m^3$ off the northern coast of Scotland for the simulation in which 120 kt/d are emitted between the surface to 1500 m altitude agl. For all other simulations and over populated areas in Northern Europe the number of consecutive hours of exposure to the 266 $\mu g/m^3$ threshold is less than 11 h. Although the observations and our model simulations show that volcanic SO_2 pollution from Icelandic flood lava eruptions can degrade air quality and pose a hazard to human health, there was no risk of long-term detrimental health effects in the far field due to the eruption because exposure to pollutants was transient and of very short duration. In Iceland, in contrast, prolonged exposure to pollution from the eruption [*Gíslason et al*., 2015] implies health risks.

4. Summary and Conclusions

With an erupted lava volume of about 1.5 km^3 [*IMO*, 2015], the 2014–2015 eruption at Holuhraun was the largest volume eruption in Iceland since the 1783–1784 C.E. Laki eruption, which erupted 14.7 ± 1.0 km^3 of lava and emitted 122 Tg of SO_2 over the course of 8 months [*Thordarson and Self*, 1993]. Lava-producing Icelandic eruptions of flood lava size (i.e., producing more than 1 km^3 of lava) are rare events with one eruption occurring every 200 to 500 years [*Thordarson and Larsen*, 2007]. However, smaller effusive Icelandic eruptions have a much higher frequency with one eruption every 40–50 years on average based on the record of eruptions in the last 1100 years [*Thordarson and Larsen*, 2007].

The continuous emission of volcanic SO_2 from the 2014–2015 eruption at Holuhraun into the lowermost troposphere presented a unique case study to test the ability of satellite remote sensing instruments to detect low-altitude volcanic SO_2 plumes over large areas. We have shown that the retrievals developed by *Theys et al*. [2015] for OMI and by *Carboni et al*. [2012] for IASI successfully detected the low-altitude SO_2 plume from the eruption throughout September 2014 (Figure 3). For September 2014, we calculate a significant daily SO_2 mass burden in the atmosphere of 99 ± 49 kt of SO_2 from OMI and 61 ± 18 kt of SO_2 from IASI on average (Figure 4 and Table S2), which is at least a factor of 2 greater than the SO_2 burden over Europe due to anthropogenic emissions in 2007–2009.

Using the Met Office's NAME model together with OMI and IASI retrievals of the SO_2 vertical column density and mass burdens, we were able to constrain the volcanic SO_2 fluxes independent of ground-based optical remote sensing measurements for September 2014. Overall, we constrain emission rates to up to 120 kt/d during early September 2014, followed by a decrease to 20–60 kt/d between 6 and 22 September 2014, followed by a renewed increase to 60–120 kt/d until the end of September 2014 (Figure 4). Based on these fluxes, we estimate that the eruption emitted a total of 2.0 ± 0.6 Tg of SO_2 into the atmosphere during September 2014, which is in good agreement with ground-based remote sensing [*Gíslason et al*., 2015] and petrological estimates [*Thordarson and Hartley*, 2015]. Our estimate of the peak flux of 120 kt/d is, however, at the lower end of the range of SO_2 fluxes estimated empirically combining lava discharge rates with petrological estimates of the SO_2 emissions for early September 2014 [*Thordarson and Hartley*, 2015].

We also show that satellite-derived and model-simulated vertical column densities of SO_2 compare reasonably well. However, model simulations are biased low by up to a factor of 8 when compared to surface observations at specific times and locations in the far field. We find that relatively small positional errors of the volcanic plume (in the horizontal and in the vertical in particular) occurring over transport distances of

thousands of kilometers and the height of the boundary layer diagnosed in the model can explain most of these biases. Overall, our results demonstrate that quantitatively predicting volcanic SO_2 mass concentrations at specific locations in the far field is challenging and subject to uncertainties in, for instance, the eruption source term, pollutant removal rates, and meteorological fields used to drive the model, which is also the case for other pollutants such as volcanic ash [*Devenish et al*., 2012a, 2012b; *Kristiansen et al*., 2012; *Webster et al*., 2012; *Dacre et al*., 2015].

Despite the eruption emitting SO_2 into the lowermost troposphere, we have also shown that volcanic SO_2 was transported over long distances and detected by air quality monitoring stations up to 2700 km away from the source (Table 2 and Figure 2). In the United Kingdom, DEFRA monitors and forecasts air quality and issues health advice in the event of air pollution exceeding pollutant-specific thresholds [*Connolly et al*., 2013]. Although the pollution episodes due to the eruption were transient in the far field (Figures 2 and 5) and volcanic eruptions are sporadic events, the monitoring sites across Northern Europe facilitated the detection and characterization of the air quality impacts due to the eruption. During the 1783–1784 C. E. Laki flood lava eruption SO_2 emission rates [*Thordarson et al*., 1996] were up to an order of magnitude greater than during the 2014–2015 eruption at Holuhraun. Differences in eruption style and emission height mean, however, that a simple linear scaling between the SO_2 emission rate at source and the observations in the far field cannot be applied. Therefore, existing air quality monitoring networks should be retained or extended to monitor SO_2 and other volcanic pollutants from future eruptions in Iceland. This would facilitate the characterization and mitigation of volcanic gas and aerosol particle hazards, which could be severe in the event of a large-magnitude Icelandic flood lava eruption [*Thordarson and Self*, 2003; *Schmidt et al*., 2011; *Loughlin et al*., 2012]. In response to the eruptions in Iceland since 2010, the Scottish Environment Protection Agency is going to extend their air quality monitoring of SO_2 and particulates [*Scottish Environment Protection Agency*, 2015]. This decision has been taken at a time when across Europe the number of SO_2 monitoring stations had been reduced as a result of successfully legislated reductions of SO_2 emissions from anthropogenic sources since the 1980s.

To improve air quality forecasting during a volcanic eruption, we recommend a systematic use of high-quality, well-documented and validated operational satellite data sets that are characterized in the vertical (i.e., column operators are made available) along with in situ data from surface air quality monitoring sites across Europe. During the eruption, ECMWF-Monitoring atmospheric composition and climate (MACC) assimilated satellite data of volcanic SO_2 to achieve a better forecast skill during mid-September 2014 [*ECMWF-MACC*, 2014]. The satellite data and air quality observations presented here also lend themselves to deriving SO_2 emission rates at high temporal resolution using inverse modeling procedures [e.g., *Boichu et al*., 2013, 2014].

Acknowledgments

A.S. received funding through an Academic Research Fellowship from the School of Earth and Environment (University of Leeds), a UK Natural Environment Research Council (NERC) grant VANAHEIM NE/I015612/1, and via the Met Office Academic Partnership. A.S., T.A.M., and E.I. are funded by a NERC urgency grant NE/M021130/1 (the source and longevity of sulphur in an Icelandic flood basalt eruption plume). A.S. is a COMET associate scientist, and T.A.M. and E.C. acknowledge COMET funding. A.S. thanks Martyn P. Chipperfield and Hans F. Graf for their very helpful discussions of this work and two anonymous reviewers for their constructive and detailed comments. We also acknowledge the National Institute for Public Health and the Environment (RIVM) for making available the air quality data for the Netherlands. The data for this paper are available upon request from the corresponding author (Anja Schmidt, a.schmidt@leeds.ac.uk).

References

Arason, Þ., H. Bjornsson, G. N. Petersen, E. B. Jónasdóttir, and B. B. Oddsson (2015), Plume height during the 2014–2015 Holuhraun volcanic eruption, *Geophys. Res.*, Abstracts, EGU2015-11498.

Beirle, S., C. Hörmann, M. Penning de Vries, S. Dörner, C. Kern, and T. Wagner (2014), Estimating the volcanic emission rate and atmospheric lifetime of SO_2 from space: A case study for Kīlauea Volcano, Hawai`i, *Atmos. Chem. Phys.*, *14*(16), 8309–8322.

Boichu, M., L. Menut, D. Khvorostyanov, L. Clarisse, C. Clerbaux, S. Turquety, and P. F. Coheur (2013), Inverting for volcanic SO_2 flux at high temporal resolution using spaceborne plume imagery and chemistry-transport modelling: The 2010 Eyjafjallajökull eruption case study, *Atmos. Chem. Phys.*, *13*(17), 8569–8584.

Boichu, M., L. Clarisse, D. Khvorostyanov, and C. Clerbaux (2014), Improving volcanic sulfur dioxide cloud dispersal forecasts by progressive assimilation of satellite observations, *Geophys. Res. Lett.*, *41*, 2637–2643, doi:10.1002/2014GL059496.

Boulon, J., K. Sellegri, M. Hervo, and P. Laj (2011), Observations of nucleation of new particles in a volcanic plume, *Proc. Natl. Acad. Sci. U.S.A.*, *108*(30), 12,223–12,226, doi:10.1073/pnas.1104923108.

Brook, R. D., et al. (2010), Particulate matter air pollution and cardiovascular disease: An update to the scientific statement from the American Heart Association, *Circulation*, *121*(21), 2331–2378.

Carboni, E., R. Grainger, J. Walker, A. Dudhia, and R. Siddans (2012), A new scheme for sulphur dioxide retrieval from IASI measurements: Application to the Eyjafjallajökull eruption of April and May 2010, *Atmos. Chem. Phys.*, *12*(23), 11,417–11,434.

Carn, S. A., N. A. Krotkov, K. Yang, and A. J. Krueger (2013), Measuring global volcanic degassing with the Ozone Monitoring Instrument (OMI), *Spec. Publ. Geol. Soc. London*, *380*(1), 229–257.

Clarisse, L., P. F. Coheur, N. Theys, D. Hurtmans, and C. Clerbaux (2014), The 2011 Nabro eruption, a SO_2 plume height analysis using IASI measurements, *Atmos. Chem. Phys.*, *14*(6), 3095–3111.

Clerbaux, C., et al. (2009), Monitoring of atmospheric composition using the thermal infrared IASI/MetOp sounder, *Atmos. Chem. Phys.*, *9*(16), 6041–6054.

Cohen, A. J., et al. (2005), The global burden of disease due to outdoor air pollution, *J. Toxicol. Environ. Health, Part A*, *68*(13–14), 1301–1307.

Collins, W. J., D. S. Stevenson, C. E. Johnson, and R. G. Derwent (1997), Tropospheric ozone in a global-scale three-dimensional Lagrangian model and its response to NOX emission controls, *J. Atmos. Chem.*, *26*(3), 223–274.

Connolly, E., G. Fuller, T. Baker, and P. Willis (2013), *Update on Implementation of the Daily Air Quality Index*, pp. 1–11, Department for Environment Food and Rural Affairs, London. [Available at http://uk-air.defra.gov.uk/library/reports?report_id=750.]

Dacre, H. F., A. L. M. Grant, N. J. Harvey, D. J. Thomson, H. N. Webster, and F. Marenco (2015), Volcanic ash layer depth: Processes and mechanisms, *Geophys. Res. Lett.*, *42*, 637–645, doi:10.1002/2014GL062454.

Davies, T., M. J. P. Cullen, A. J. Malcolm, M. H. Mawson, A. Staniforth, A. A. White, and N. Wood (2005), A new dynamical core for the Met Office's global and regional modelling of the atmosphere, *Q. J. R. Meteorol. Soc.*, *131*(608), 1759–1782.

Derwent, R. G., P. G. Simmonds, A. J. Manning, and T. G. Spain (2007), Trends over a 20-year period from 1987 to 2007 in surface ozone at the atmospheric research station, Mace Head, Ireland, *Atmos. Environ.*, *41*(39), 9091–9098.

Devenish, B. J., P. N. Francis, B. T. Johnson, R. S. J. Sparks, and D. J. Thomson (2012a), Sensitivity analysis of dispersion modeling of volcanic ash from Eyjafjallajökull in May 2010, *J. Geophys. Res.*, *117*, D00U21, doi:10.1029/2011JD016782.

Devenish, B. J., D. J. Thomson, F. Marenco, S. J. Leadbetter, H. Ricketts, and H. F. Dacre (2012b), A study of the arrival over the United Kingdom in April 2010 of the Eyjafjallajökull ash cloud using ground-based lidar and numerical simulations, *Atmos. Environ.*, *48*, 152–164.

Dürig, T., M. Gudmundsson, T. Högnadóttir, I. Jónsdóttir, S. Gudbjörnsson, Ö. Lárusson, Á. Höskuldsson, T. Thordarson, M. Riishuus, and E. Magnússon (2015), Estimation of lava flow field volumes and volumetric effusion rates from airborne radar profiling and other data: Monitoring of the Nornahraun (Holuhraun) 2014/15 eruption in Iceland, *Geophys. Res.*, Abstracts, 17, EGU2015-8519-2012.

ECMWF-MACC (2014), MACC-III supports French authorities on elevated SO_2 values.

European Environmental Agency (EEA) (2013), *Air Quality in Europe—2013 Report*, 107 pp., European Environmental Agency, Copenhagen, Den., doi:10.2800/92843.

European Environmental Agency (EEA) (2014), Emission trends of sulphur oxides in EU-28 group of countries, 2015 (Last accessed on: 11 January). [Available at http://www.eea.europa.eu/data-and-maps/daviz/emission-trends-of-sulphur-oxides#tab-chart_1.]

Elias, T., and A. J. Sutton (2012), Sulfur dioxide emission rates from Kīlauea Volcano, Hawai'i, 2007–2010, *U.S. Geol. Surv. Open File Rep., 2012–1107,* 25 pp. [Available at http://pubs.usgs.gov/of/2012/1107_text.pdf.]

Gíslason, S. R., et al. (2015), Environmental pressure from the 2014–15 eruption of Bárðarbunga volcano, Iceland, *Geochem. Perspect. Lett.*, *1*, 84–93.

Gudmundsson, A., N. Lecoeur, N. Mohajeri, and T. Thordarson (2014), Dike emplacement at Bardarbunga, Iceland, induces unusual stress changes, caldera deformation, and earthquakes, *Bull. Volcanol.*, *76*(10), 1–7.

Hansell, A., and C. Oppenheimer (2004), Health hazards from volcanic gases: A systematic literature review, *Arch. Environ. Health*, *59*(12), 628–639.

Hartley, M. E., and T. Thordarson (2013), The 1874–1876 volcano-tectonic episode at Askja, North Iceland: Lateral flow revisited, *Geochem. Geophys. Geosyst.*, *14*, 2286–2309, doi:10.1002/ggge.20151.

Heard, I. P. C., A. J. Manning, J. M. Haywood, C. Witham, A. Redington, A. Jones, L. Clarisse, and A. Bourassa (2012), A comparison of atmospheric dispersion model predictions with observations of SO_2 and sulphate aerosol from volcanic eruptions, *J. Geophys. Res.*, *117*, D00U22, doi:10.1029/2011JD016791.

Höskuldsson, Á., I. Jónsdóttir, M. S. Riishus, G. B. M. Pedersen, M. T. Gudmundsson, T. Thordarson, V. Drouin, and Futurevolc IES field work team (2015), Magma discharge and lava flow field growth in the Nornahraun/Bardarbunga eruption Iceland, *Geophys. Res.*, Abstracts, 17, EGU2015-12755-2.

Ialongo, I., J. Hakkarainen, R. Kivi, P. Anttila, N. A. Krotkov, K. Yang, C. Li, S. Tukiainen, S. Hassinen, and J. Tamminen (2015), Validation of satellite SO_2 observations in northern Finland during the Icelandic Holuhraun fissure eruption, *Atmos. Meas. Tech. Discuss.*, *8*(1), 599–621.

Icelandic Met Office (IMO) (2014), *100 Days of Continuous Eruptive Activity in Holuhraun*, Icelandic Met Office, Iceland. [Available at http://en.vedur.is/media/jar/bb100days_ens.pdf.]

Icelandic Met Office (IMO) (2015), Bárðarbunga 2014–2015 updates, 2015 (Last accessed on: 3 March). [Available at http://en.vedur.is/earthquakes-and-volcanism/articles/nr/3000#ag31.]

Jones, A. R., D. J. Thomson, M. Hort, and B. Devenish (2007), The U.K. Met Office's next-generation atmospheric dispersion model, NAME III, in *Air Pollution Modeling and Its Application XVII (Proceedings of the 27th NATO/CCMS International Technical Meeting on Air Pollution Modelling and Its Application),* edited by C. Borrego and A.-L. Norman, pp. 580–589, Springer, Utrecht, Netherlands.

Kazahaya, K., H. Shinohara, K. Uto, M. Odai, Y. Nakahori, H. Mori, H. Iino, M. Miyashita, and J. Hirabayashi (2004), Gigantic SO_2 emission from Miyakejima volcano, Japan, caused by caldera collapse, *Geology*, *32*(5), 425–428.

Kristiansen, N. I., et al. (2012), Performance assessment of a volcanic ash transport model mini-ensemble used for inverse modeling of the 2010 Eyjafjallajökull eruption, *J. Geophys. Res.*, *117*, D00U11, doi:10.1029/2011JD016844.

Leadbetter, S. J., and M. C. Hort (2011), Volcanic ash hazard climatology for an eruption of Hekla Volcano, Iceland, *J. Volcanol. Geotherm. Res.*, *199*(3–4), 230–241.

Leadbetter, S. J., M. C. Hort, S. von Löwis, K. Weber, and C. S. Witham (2012), Modeling the resuspension of ash deposited during the eruption of Eyjafjallajökull in spring 2010, *J. Geophys. Res.*, *117*, D00U10, doi:10.1029/2011JD016802.

Leadbetter, S. J., M. C. Hort, A. R. Jones, H. N. Webster, and R. R. Draxler (2015), Sensitivity of the modelled deposition of Caesium-137 from the Fukushima Dai-ichi nuclear power plant to the wet deposition parameterisation in NAME, *J. Environ. Radioact.*, *139*, 200–211.

Lee, C., R. V. Martin, A. van Donkelaar, G. O'Byrne, N. Krotkov, A. Richter, L. G. Huey, and J. S. Holloway (2009), Retrieval of vertical columns of sulfur dioxide from SCIAMACHY and OMI: Air mass factor algorithm development, validation, and error analysis, *J. Geophys. Res.*, *114*, D22303, doi:10.1029/2009JD012123.

Lee, C., R. V. Martin, A. van Donkelaar, H. Lee, R. R. Dickerson, J. C. Hains, N. Krotkov, A. Richter, K. Vinnikov, and J. J. Schwab (2011), SO_2 emissions and lifetimes: Estimates from inverse modeling using in situ and global, space-based (SCIAMACHY and OMI) observations, *J. Geophys. Res.*, *116*, D06304, doi:10.1029/2010JD014758.

Levelt, P. F., G. H. J. van den Oord, M. R. Dobber, A. Malkki, V. Huib, J. de Vries, P. Stammes, J. O. V. Lundell, and H. Saari (2006), The Ozone Monitoring Instrument, *IEEE Trans. Geosci. Remote Sens.*, *44*(5), 1093–1101.

Longo, B. M. (2013), Adverse health effects associated with increased activity at Kīlauea Volcano: A repeated population-based survey, *ISRN Public Health*, 2013, 10.

Longo, B. M., A. Rossignol, and J. B. Green (2008), Cardiorespiratory health effects associated with sulphurous volcanic air pollution, *Public Health*, *122*(8), 809–820.

Longo, B. M., W. Yang, J. B. Green, F. L. Crosby, and V. L. Crosby (2010), Acute health effects associated with exposure to volcanic air pollution (vog) from increased activity at Kilauea Volcano in 2008, *J. Toxicol. Environ. Health, Part A*, *73*(20), 1370–1381.

Loughlin, S. C., W. P. A. Aspinall, C. Vye-Brown, P. J. Baxter, C. Braban, M. Hort, A. Schmidt, T. Thordarson, and C. S. Witham (2012), Large-magnitude fissure eruptions in Iceland: Source characterisation, British Geol. Surv. Open File Rep., OR/12/098. [Available at www.bgs.ac.uk/downloads/start.cfm?id=2881.]

McCormick, B. T., M. Herzog, J. Yang, M. Edmonds, T. A. Mather, S. A. Carn, S. Hidalgo, and B. Langmann (2014), A comparison of satellite- and ground-based measurements of SO_2 emissions from Tungurahua volcano, Ecuador, *J. Geophys. Res. Atmos.*, *119*, 4264–4285, doi:10.1002/2013JD019771.

Platt, U., and J. Stutz (2008), *Differential Optical Absorption Spectroscopy (DOAS): Principle and Applications*, Springer, Berlin.

Pope, C. A., and D. W. Dockery (2006), Health effects of fine particulate air pollution: Lines that connect, *J. Air Waster Manage. Assoc.*, *56*(6), 709–742.

Pope, C. A., R. T. Burnett, M. J. Thun, E. E. Calle, D. Krewski, K. Ito, and G. D. Thurston (2002), Lung cancer, cardiopulmonary mortality, and long-term exposure to fine particulate air pollution, *J. Am. Med. Assoc.*, *287*(9), 1132–1141.

Rall, D. P. (1974), Review of the health effects of sulfur oxides, *Environ. Health Perspect.*, *8*, 97–121.

Redington, A. L., R. G. Derwent, C. S. Witham, and A. J. Manning (2009), Sensitivity of modelled sulphate and nitrate aerosol to cloud, pH and ammonia emissions, *Atmos. Environ.*, *43*(20), 3227–3234.

Salerno, G. G., M. R. Burton, C. Oppenheimer, T. Caltabiano, D. Randazzo, N. Bruno, and V. Longo (2009), Three-years of SO_2 flux measurements of Mt. Etna using an automated UV scanner array: Comparison with conventional traverses and uncertainties in flux retrieval, *J. Volcanol. Geotherm. Res.*, *183*(1–2), 76–83.

Schmidt, A., K. S. Carslaw, G. W. Mann, M. Wilson, T. J. Breider, S. J. Pickering, and T. Thordarson (2010), The impact of the 1783–1784 AD Laki eruption on global aerosol formation processes and cloud condensation nuclei, *Atmos. Chem. Phys.*, *10*(13), 6025–6041.

Schmidt, A., B. Ostro, K. S. Carslaw, M. Wilson, T. Thordarson, G. W. Mann, and A. J. Simmons (2011), Excess mortality in Europe following a future Laki-style Icelandic eruption, *Proc. Natl. Acad. Sci. U.S.A.*, *108*(38), 15,710–15,715.

Schmidt, A., T. Thordarson, L. D. Oman, A. Robock, and S. Self (2012a), Climatic impact of the long-lasting 1783 Laki eruption: Inapplicability of mass-independent sulfur isotopic composition measurements, *J. Geophys. Res.*, *117*, D23116, doi:10.1029/2012JD018414.

Schmidt, A., K. S. Carslaw, G. W. Mann, A. Rap, K. J. Pringle, D. V. Spracklen, M. Wilson, and P. M. Forster (2012b), Importance of tropospheric volcanic aerosol for indirect radiative forcing of climate, *Atmos. Chem. Phys.*, *12*(16), 7321–7339.

Schmidt, A., et al. (2014), Assessing hazards to aviation from sulfur dioxide emitted by explosive Icelandic eruptions, *J. Geophys. Res. Atmos.*, *119*, 14,180–14,196, doi:10.1002/2014JD022070.

Scottish Environment Protection Agency (2015), Watching the Icelandic volcanoes, 2015 (Last accessed on: 25 March). [Available at http://www.sepaview.com/2015/03/watching-the-icelandic-volcanoes/.]

Sigmundsson, F., et al. (2015), Segmented lateral dyke growth in a rifting event at Bárðarbunga volcanic system, Iceland, *Nature*, *517*(7533), 191–195.

Stevenson, D. S., C. E. Johnson, W. J. Collins, and R. G. Derwent (2003), The tropospheric sulphur cycle and the role of volcanic SO_2, *Volcanic Degassing*, *6*(213), 295–305.

Support to Aviation Control Service (2014), 6 September 2014 SACS SO_2 notification on website, (Last accessed on: 6 September 2014). [Available at http://sacs.aeronomie.be/nrt/index.php?Year=2014&Month=09&Day=06&Region=105&InstruGOME2=1&InstruOMI=0&InstruIASI=0&InstruIASIb=0&InstruAIRS=0&plum=&obsVCD=1&obsAAI=2&obsCCF=0.]

Theys, N., et al. (2015), Sulfur dioxide vertical column DOAS retrievals from the Ozone Monitoring Instrument: Global observations and comparison to ground-based and satellite data, *J. Geophys. Res. Atmos.*, *120*, 2470–2491, doi:10.1002/2014JD022657.

Thordarson, T., and M. Hartley (2015), Atmospheric sulfur loading by the ongoing Nornahraun eruption, North Iceland, *Geophys. Res.*, Abstracts, 17(EGU2015-10708).

Thordarson, T., and G. Larsen (2007), Volcanism in Iceland in historical time: Volcano types, eruption styles and eruptive history, *J. Geodyn.*, *43*(1), 118–152.

Thordarson, T., and S. Self (1993), The Laki (Skaftar Fires) and Grimsvötn eruptions in 1783–1785, *Bull. Volcanol.*, *55*(4), 233–263.

Thordarson, T., and S. Self (2003), Atmospheric and environmental effects of the 1783–1784 Laki eruption: A review and reassessment, *J. Geophys. Res.*, *108*(D1), 4011, doi:10.1029/2001JD002042.

Thordarson, T., S. Self, N. Oskarsson, and T. Hulsebosch (1996), Sulfur, chlorine, and fluorine degassing and atmospheric loading by the 1783–1784 AD Laki (Skaftar fires) eruption in Iceland, *Bull. Volcanol.*, *58*(2–3), 205–222.

Tu, F. H., D. C. Thornton, A. R. Bandy, G. R. Carmichael, Y. Tang, K. L. Thornhill, G. W. Sachse, and D. R. Blake (2004), Long-range transport of sulfur dioxide in the central Pacific, *J. Geophys. Res.*, *109*, D15S08, doi:10.1029/2003JD004309.

Turnock, S. T., et al. (2015), Modelled and observed changes in aerosols and surface solar radiation over Europe between 1960 and 2009, *Atmos. Chem. Phys.*, *15*, 9477–9500, doi:10.5194/acp-15-9477-2015.

Umweltbundesamt (2014), Monatsbericht Hintergrundmessnetz Umweltbundesamt September 2014, 31 pp., Wien.

U.S. Geological Survey (USGS) (2013), The ongoing Pu'u 'Ō'ō eruption of Kīlauea Volcano, Hawai'i—30 years of eruptive activity, *U.S. Geol. Surv. Open File Rep.*, 1–6 pp. [Available at http://pubs.usgs.gov/fs/2012/3127/.]

Walker, J. C., A. Dudhia, and E. Carboni (2011), An effective method for the detection of trace species demonstrated using the MetOp Infrared Atmospheric Sounding Interferometer, *Atmos. Meas. Tech.*, *4*(8), 1567–1580.

Walker, J. C., E. Carboni, A. Dudhia, and R. G. Grainger (2012), Improved detection of sulphur dioxide in volcanic plumes using satellite-based hyperspectral infrared measurements: Application to the Eyjafjallajökull 2010 eruption, *J. Geophys. Res.*, *117*, D00U16, doi:10.1029/2011JD016810.

Webster, H. N., and D. J. Thomson (2011), Dry deposition modelling in a Lagrangian dispersion model, *Int. J. Environ. Pollut.*, *47*(1), 1–9.

Webster, H. N., and D. J. Thomson (2014), The NAME wet deposition scheme, *Forecasting Res. Tech. Rep. 584*, 43.

Webster, H. N., D. J. Thomson, and N. L. Morrison (2003), New turbulence profiles for NAME, UK Met Office turbulence and diffusion note 288.

Webster, H. N., S. J. Abel, J. P. Taylor, D. J. Thomson, J. M. Haywood, M. C. Hort, and Hadley (2006), Dispersion modelling studies of the Buncefield oil depot incident, *Centre Tech. Note, 69*, Met Office, Exeter.

Webster, H. N., et al. (2012), Operational prediction of ash concentrations in the distal volcanic cloud from the 2010 Eyjafjallajökull eruption, *J. Geophys. Res.*, *117*, D00U08, doi:10.1029/2011JD016790.

World Health Organization (WHO) (2008), The global burden of disease: 2004 update. [Available at http://www.who.int/healthinfo/global_burden_disease/GBD_report_2004update_full.pdf.]

World Health Organization (WHO) (2014), Ambient (outdoor) air quality and health, Fact sheet N°313.

Witham, C., H. Webster, M. Hort, A. Jones, and D. Thomson (2012), Modelling concentrations of volcanic ash encountered by aircraft in past eruptions, *Atmos. Environ.*, *48*, 219–229.

Yuan, T., L. A. Remer, and H. Yu (2011), Microphysical, macrophysical and radiative signatures of volcanic aerosols in trade wind cumulus observed by the A-Train, *Atmos. Chem. Phys.*, *11*(14), 7119–7132.

Zentralanstalt für Meteorologie und Geodynamik (2014), Hohe SO_2-Werte in Teilen Österreichs durch isländischen Vulkan, 2014 (Last accessed on: 25 September). [Available at http://www.zamg.ac.at/cms/de/umwelt/news/hohe-so2-in-teilen-oesterreichs-durch-islaendischen-vulkan.]